



2013

CAMBER CONTROL IN SIMPLY SUPPORTED PRESTRESSED CONCRETE BRIDGE GIRDERS

Osamah Ibrahim Mahmood
University of Kentucky, oima222@uky.edu

[Click here to let us know how access to this document benefits you.](#)

Recommended Citation

Mahmood, Osamah Ibrahim, "CAMBER CONTROL IN SIMPLY SUPPORTED PRESTRESSED CONCRETE BRIDGE GIRDERS" (2013). *Theses and Dissertations--Civil Engineering*. 7.
https://uknowledge.uky.edu/ce_etds/7

This Master's Thesis is brought to you for free and open access by the Civil Engineering at UKnowledge. It has been accepted for inclusion in Theses and Dissertations--Civil Engineering by an authorized administrator of UKnowledge. For more information, please contact UKnowledge@lsv.uky.edu.

STUDENT AGREEMENT:

I represent that my thesis or dissertation and abstract are my original work. Proper attribution has been given to all outside sources. I understand that I am solely responsible for obtaining any needed copyright permissions. I have obtained and attached hereto needed written permission statements(s) from the owner(s) of each third-party copyrighted matter to be included in my work, allowing electronic distribution (if such use is not permitted by the fair use doctrine).

I hereby grant to The University of Kentucky and its agents the non-exclusive license to archive and make accessible my work in whole or in part in all forms of media, now or hereafter known. I agree that the document mentioned above may be made available immediately for worldwide access unless a preapproved embargo applies.

I retain all other ownership rights to the copyright of my work. I also retain the right to use in future works (such as articles or books) all or part of my work. I understand that I am free to register the copyright to my work.

REVIEW, APPROVAL AND ACCEPTANCE

The document mentioned above has been reviewed and accepted by the student's advisor, on behalf of the advisory committee, and by the Director of Graduate Studies (DGS), on behalf of the program; we verify that this is the final, approved version of the student's dissertation including all changes required by the advisory committee. The undersigned agree to abide by the statements above.

Osamah Ibrahim Mahmood, Student

Dr. Issam Harik, Major Professor

Dr. Kaymar C. Mahboub, Director of Graduate Studies

CAMBER CONTROL IN SIMPLY SUPPORTED PRESTRESSED CONCRETE
BRIDGE GIRDERS

THESIS

A thesis submitted in partial fulfillment of the
requirements for the degree of Master of Science in Civil Engineering in the
College of Engineering
at the University of Kentucky

By

Osamah Ibrahim Mahmood

Lexington, Kentucky

Director: Dr. Issam Elias Harik, Professor of Civil Engineering

Lexington, Kentucky

2013

Copyright © Osamah Ibrahim Mahmood 2013

ABSTRACT OF THESIS

CAMBER CONTROL IN SIMPLY SUPPORTED PRESTRESSED CONCRETE BRIDGE GIRDERS

When designing a bridge, serviceability usually controls and is a more important factor than the ultimate capacity of the bridge or the allowable stresses. Therefore, the behavior of the bridge girder deflection and camber must be predicted as accurately as possible. Therefore, excessive camber has become one of the most common problems when constructing concrete bridges. Different methods have been developed to overcome this problem. The most common and widely used is using haunch with adjustable pedestals to overcome the excessive camber. However, this method has limitations that must be considered. Therefore, this study is evaluating the effectiveness of using post tensioning jacking strands at the top flange of simply supported bridge girders to reduce the excessive camber and make it equal to the design camber.

KEYWORDS: Camber, Camber Control

Osamah Ibrahim Mahmood

May 3, 2013

CAMBER CONTROL IN SIMPLY SUPPORTED PRESTRESSED CONCRETE
BRIDGE GIRDERS

By

Osamah Ibrahim Mahmood

Dr. Issam Elias Harik

Director of Dissertation

Dr. Kamyar C.Mahboub

Director of Graduate Studies

May 3, 2013

ACKNOWLEDGMENTS

This thesis would not have been possible without the help, patience, and support of my supervisor, Prof. Issam Harik. The invaluable good advice, and support on both an academic and personal level. For which I am extremely grateful.

I thank my parents, brothers, sisters, and friends for keeping me in their prayers.

TABLE OF CONTENTS

Acknowledgments.....	iii
List of Figures.....	iv
Chapter 1 INTRODUCTION	1
1.1 Introduction	1
1.2 Research Objective	3
1.3 Research Tasks	3
1.4 Research Significance	3
1.5 Organization of the Thesis	4
Chapter 2 LITERATURE REVIEW	5
2.1 Introduction	5
2.2 Haunch Components	5
2.3 Maximum and Minimum Haunch Values	5
2.4 Summary	6
Chapter 3 MATERIAL PROPERTIES	7
3.1 Introduction	7
3.2 Concrete	7
3.3 Mild Steel	10
3.4 Prestressing Steel	11
3.5 Summary	13
Chapter 4 MOMENT- CURVATURE DIAGRAM OF PRESTRESSED CONCRETE BRIDGE GIRDERS	14
4.1 Introduction	14
4.2 Basic Assumptions	14
4.3 Prestressed Concrete Bridge Girders Cross Sectional Moment	15
4.3.1 Concrete Forces	15

4.3.1.1	Concrete Compressive Forces	15
4.3.1.2	Concrete Tensile Forces	17
4.3.2	Mild Steel Reinforcement Forces	19
4.3.3	Pretensioning Steel Forces	20
4.3.4	Post tensioning Steel Used to Control Camber Forces	21
4.3.5	Moment -Curvature ($M \phi$)	23
4.4	Summary	23
Chapter 5	CAMBER CONTROL	26
5.1	Introduction	26
5.2	Basic Assumptions	26
5.3	Initial Camber	26
5.4	Design Camber	30
5.5	Example	41
5.6	Moment Capacity Reduction	43
5.7	Example	47
Chapter 6	CONCLUSIONS AND RECOMMENDATIONS	48
6.1	Conclusion and Findings	48
6.2	Future Work	48
Appendix A		49
Appendix B	NOTATION	71
References		73
Vita		76

LIST OF FIGURES

Fig. 1.1	Typical camber adjustment details	2
Fig. 3.1	Concrete stress-strain relationships Modified Hognestad model for (a) compression and (b) tension	8
Fig. 3.2	Modified CALTRANS stress-strain relationship for Grade 60 steel	10
Fig. 3.3	Stress-strain relationships of 7-wire low relaxation prestressing steel strands	13
Fig. 4.1	Rectangular beam cross section and reinforcement details	15
Fig. 4.2	(a) Concrete compression side strips, (b) strain distribution, (c) stresses and (d)) concrete stresses at reinforcement layers	17
Fig. 4.3	(a) Concrete tension side strips, (b) strain distribution, (c) stresses and (d)) concrete stresses at reinforcement layers	18
Fig. 4.4	(a) Mild steel layouts, (b) strain distribution, (c) stresses and (d) forces	19
Fig. 4.5	(a) Pretensioning steel layout, (b) strain distribution, (c) stresses and (d) forces	20
Fig. 4.6	(a) Post tensioning steel layout, (b) strain distribution, (c) stresses and (d) forces	22
Fig. 4.7a	Bilinear Moment- Curvature, $M-\phi$, interaction diagram the PCI 8 girder	24
Fig. 4.7b	Bilinear Load-Deflection, $P-\Delta$, interaction diagram the PCI 8 girder	25
Fig. 5.1	(a) Forces and (b) strain distributions in rectangular concrete beam due to effective pretensioning force only	27
Fig. 5.2	(a) Prestressed beam pretensioning strand profile,(b) curvature, and (c) elastic curve for singly supported bridge girder with double depression point	29
Fig. 5.3	(c) Strain distributions in rectangular concrete beam due to (a) effective pretensioning force, P_e and (b) post tensioning force, P_p	30
Fig. 5.4	Variation of post tensioning Jacking force, P_p , with design camber, Δ_d ,for different pretensioning losses, T_L , for the PCI-8 girder	31

Fig. 5.5	Post tensioning Jacking force, P_p , vs. design camber, Δ_d , for different specified concrete strength, f'_c , for the PCI-8 girder	32
Fig.5.6	Post tensioning Jacking force, P_p , vs. design camber, Δ_d , for different bridge girder length, L , for the PCI-8 girder	33
Fig.5.7	Variation of post tensioning Jacking force, P_p , with design camber, Δ_d , with different distance coefficient, α , for the PCI-8 girder	34
Fig. 5.8	Comparison between results obtained from the study and Eq.5-12 for different pretensioning losses, T_L , for the PCI-8 girder	37
Fig. 5.9	Comparison between results obtained from the study and Eq.5-12 for different specified concrete compressive strength, f'_c , for the PCI-8 girder	38
Fig. 5.10	Comparison between results obtained from the study and Eq.5-12 for different bridge girder length, L , for the PCI-8 girder	39
Fig. 5.11	Comparison between results obtain from the study and from Eq.5.12 with different distance coefficient, α , for the PCI-8 girder	40
Fig. 5.12	Example details	41
Fig. 5.13	Variation of post tensioning Jacking force, P_p , with design camber, Δ_d , for pretensioning losses, $T_L=15\%$, for the PCI-8 girder	42
Fig. 5.14	Moment- curvature, $M-\phi$, interaction diagram for different post tensioning jacking force, P_p , for the PCI 8 girder	43
Fig. 5.15	Moment- curvature, $M-\phi$, interaction diagram for different post tensioning jacking force, P_p , for the PCI 8 girder	44
Fig. 5.16	Moment vs. the strain of the outermost layer of pretensioning, $M-\epsilon_{psN}$, relationship for different post tensioning jacking force, P_p , for the PCI 8 girder	45
Fig. 5.17	Moment vs. the strain of the outermost layer of pretensioning, $M-\epsilon_{psN}$, relationship for different post tensioning jacking force, P_p , for the PCI 8 girder	46

CHAPTER 1

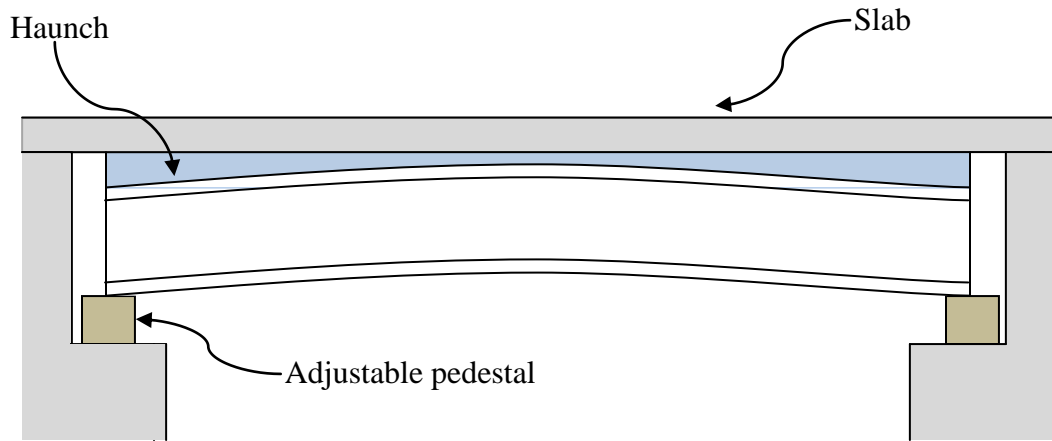
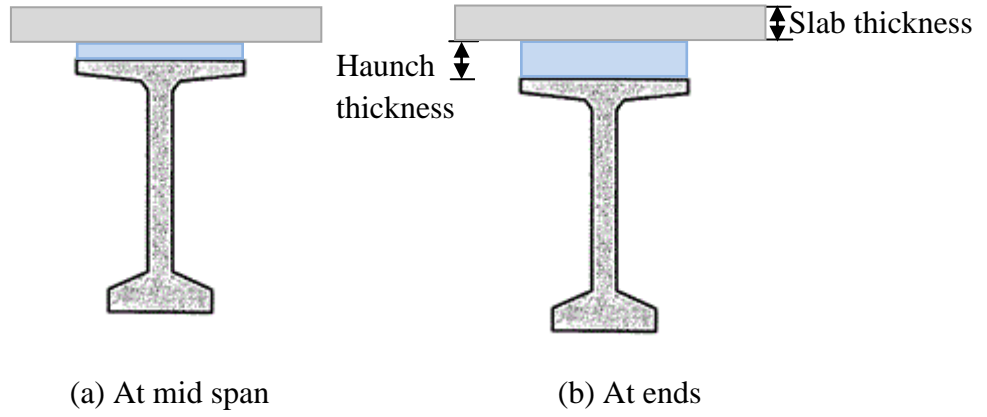
INTRODUCTION

1.1 Introduction

Prestressed concrete has passed far beyond the development stage and has established itself as a major structural material (Naaman.2004). When designing a bridge, serviceability usually controls and is a more important factor than the ultimate capacity of the bridge or the allowable stresses. Therefore, the behavior of the bridge girder deflection and camber must be predicted as accurately as possible.

Camber in prestressing concrete bridge girders is the upward deflection that is caused due to the prestressing forces applied on the bridge girder. Engineers have been trying to predict its amount and optimize it to make it vanish when placing the deck of the bridge. However, camber is affected by many factors, most of which are time dependent like creep, shrinkage, and prestress losses, causing camber to grow. This growth will lead to an excessive camber causing differential camber. Many problems will be presented due to differential camber such as: increasing haunch depths, jutting of bridge girders into the bottom of the slab and increase in time for setting up the forms for deck slabs, cracking, ride and overall performance of the bridge. Also, for adjacent box girders and deck bulb-tees, the difference in camber causes problems during the fit up process. This unnecessarily increases the time and cost of construction (Sethi.2006).

The current state of literature deals with excessive camber by adjusting the height of the haunch over the length of the bridge girder. Adjustable pedestals will be used to overcome the difference between the elevation of the bridge and the road Fig.1.1, and in some cases by adjusting the thickness of the slab. No other methods have been reported.



(c)

Figure 1.1 Typical camber adjustment details

1.2 Research Objective

The objective of this research is to evaluate the effectiveness of reducing excessive camber in simply supported prestressed concrete bridge girders prior to placement of the deck by introducing post tensioning strands in the top flange.

1.3 Research Tasks

In order to achieve the objective of this research, the following tasks will be carried out:

Task 1: Literature Review

Task 2: Material Properties

Task 3: Moment-Curvature Diagram of Prestressed Concrete Bridge Girders

Task 4: Camber Control

1.4 Research Significance

This research is trying to provide a simple and more efficient solution for the excessive camber prior to deck placement in simply supported concrete bridge girders without the need to delay the construction process, applying extra dead load to the bridge, or changing the elevation of the bridge using adjustable pedestal. This study introduces the idea of using post tensioning strands at the top flange of the bridge girder. These strands will be placed through preexisting ducts and they will be post tensioned to a certain level to reduce the initial camber and make it equal to the design camber.

1.5 Organization of the Thesis

This thesis is divided into six chapters:

- Chapter one is an introduction about the study
- Chapter two introduces the literature review dealing with excessive camber
- Chapter three presents the material properties by introducing the strain-stress relations for concrete, mild steel, and prestressing steel in order to fully understand the behavior of those materials
- Chapter four presents the analytical procedure as well as the method of analysis to generate moment-curvature diagrams in prestressed concrete bridge girders
- Chapter five presents the analytical procedure and the method of analysis to compute the camber in prestressed concrete bridge girders and explain the idea of using post tensioning to reduce camber
- Chapter six provides the overall summary and conclusions of the study. Research areas are also identified and proposed for future study

CHAPTER 2

LITERATURE REVIEW

2.1 Introduction

The current state of literature deals with excessive camber by adjusting the depth of the haunch over the length of the bridge girder, and in some cases by adjusting the thickness of the slab. No other methods have been reported. However, the first method is considered the most common approach. Therefore, this chapter presents the outlines for using haunch to reduce excessive camber.

2.2 Haunch Components

The concept behind using a haunch when controlling camber is to apply the minimum possible weight to generate a downward deflection that counteracts the effect of excessive camber. Haunch depth depends on several components: camber and camber growth, dead load of the slab, super elevation, and vertical curves of the road (Texas Department of Transportation, 2010).

2.3 Maximum and Minimum Haunch Values

Haunch limitations on I-beam are (Texas Department of Transportation, 2010):

- 1- The maximum haunch without reinforcing is 3”
- 2- The minimum haunch at the center of bearing is 1”
- 3- The minimum haunch at midspan is 0.5”

2.4 Summary

The current approach used to control camber is dependent on several factors that might control the required depth of the haunch; also, this method has limitations that might restrict the use of it regardless of the extra time and cost spent setting up forms for the haunch. Therefore, a simpler and more efficient approach is needed.

CHAPTER 3

MATERIAL PROPERTIES

3.1 Introduction

In order to understand the behavior of the materials of which the prestressed concrete bridge girder consists, this chapter will present the stress-strain relations for concrete, mild steel and prestressing steel and the necessary equations needed to compute the stresses.

3.2 Concrete

Concrete is a versatile composite material of very complex nature, yet it can be approached at any desired level of sophistication. The simplest is when only its compressive strength is specified for design. Concrete is made by mixing several components, mainly water, cement and aggregate (fine and coarse). The behavior of concrete is usually non linear. However, a standard stress-strain curve of concrete with normal weight is uniaxial. The curve consists of two main parts: an ascending portion up to the peak point which represents the maximum stress f'_c and a descending portion. In this study, the short term concrete compression stress-strain relation that is adopted is the one suggested by Hognestad (Hognestad, 1952) for short term monotonic. This stress-strain relationship is presented in Fig. 3.1a. The ascending portion is presented by Eq. 3.1 and the descending portion, which is linear, is expressed by Eq. 3.2.

$$f_c = k_3 f'_c (2\eta - \eta^2) \quad 0 \leq \varepsilon_c \leq \varepsilon_o \quad \text{Eq. 3.1}$$

$$f_c = k_3 f'_c [1 - m(\varepsilon_c - \varepsilon_o)] \quad \varepsilon_o < \varepsilon_c \leq \varepsilon_{cu} \quad \text{Eq. 3.2}$$

$$\varepsilon_o = \frac{1.7 f'_c}{E_c} \quad \text{Eq. 3.3}$$

$$\eta = \frac{\epsilon_c}{\epsilon_o} \quad \text{Eq.3.4}$$

$$k_3 = 0.85 \quad \text{Eq.3.5}$$

f_c is the concrete stress in compression corresponding to strain level ϵ_c . m is the slope of the linear part of the curve and it is to be taken as 20 to match the experimental results of cylinder tests (Ford.1981). ϵ_{cu} is the concrete compression strain at ultimate condition and it will be taken as 0.003 in/in (mm/mm) as ACI 318-11 section 10.3.2 recommends. ϵ_o is the concrete compression strain corresponding to the maximum concrete compression stress f'_c . η is the ratio of ϵ_c to ϵ_o . k_3 is represented in Eq.3.5 (Hognestad.1955).

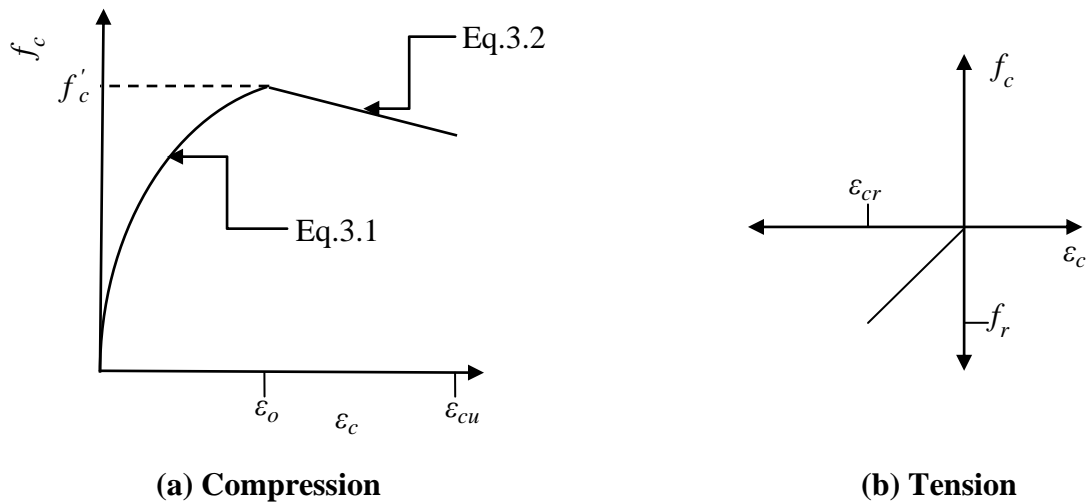


Figure 3.1 Concrete stress-strain relationships Modified Hognestad model for (a) compression and (b) tension

At low compressive stress levels ($f_c < 0.45 f'_c$), the stress-strain relationship can be assumed to be linear.

Since this study focuses on the behavior of concrete prestressed bridge girders prior to the deck placement in the field, the tension side of the cross section must be accounted for in order to obtain precise results. This study will assume concrete behaves linearly at the stage prior to cracking. The stress at concrete can be calculated using Hooks law Eq.3.7.

$$f_t = E_c \varepsilon_c \quad \text{Eq.3.7}$$

Where f_t is the concrete stress in tension corresponding to strain level ε_c . The ACI 318-11 formula to compute the tensile capacity of the concrete is adapted in this study Eq.3.8.a and Eq.3.8.b.

$$f_r = 7.5\sqrt{f'_c} \quad \text{psi} \quad \text{Eq.3.8a}$$

$$f_r = 0.7\sqrt{f'_c} \quad \text{MPa} \quad \text{Eq.3.8b}$$

f_r is the modulus of rupture of concrete (psi or MPa).

E_c is the secant modulus of elasticity of concrete determined at a service stress of $0.45f'_c$. ACI 318-11 Section 8.5.1 gives the following expression for calculating E_c .

$$E_c = 33w^{1.5}\sqrt{f'_c} \quad \text{psi} \quad \text{Eq.3.9a}$$

$$E_c = 0.043w^{1.5}\sqrt{f'_c} \quad \text{MPa} \quad \text{Eq.3.9b}$$

Where w is the volumetric weight of the concrete in lb/ft³ or kg/m³. In this study, w for normal- concrete weight is to be taken ($w=145$ lb/ft³).

3.3 Mild Steel

The behavior of mild steel offers a number of simplifications when compared to concrete. Mainly steel has the same modulus of elasticity, linear elastic portion in their stress-strain relationship, and manufactured under strict quality control that satisfies a number of ASTM standards. As a result, little variability happens between specified properties and the nature of the material. In this study, the CALTRANS mild steel stress-strain modified model for grade 60 will be used and its properties are shown in Fig.3.2. Also, it is assumed that mild steel behaves similarly under tension and compression stresses; therefore the same model will be used to compute the tensile and compressive stresses in the steel.

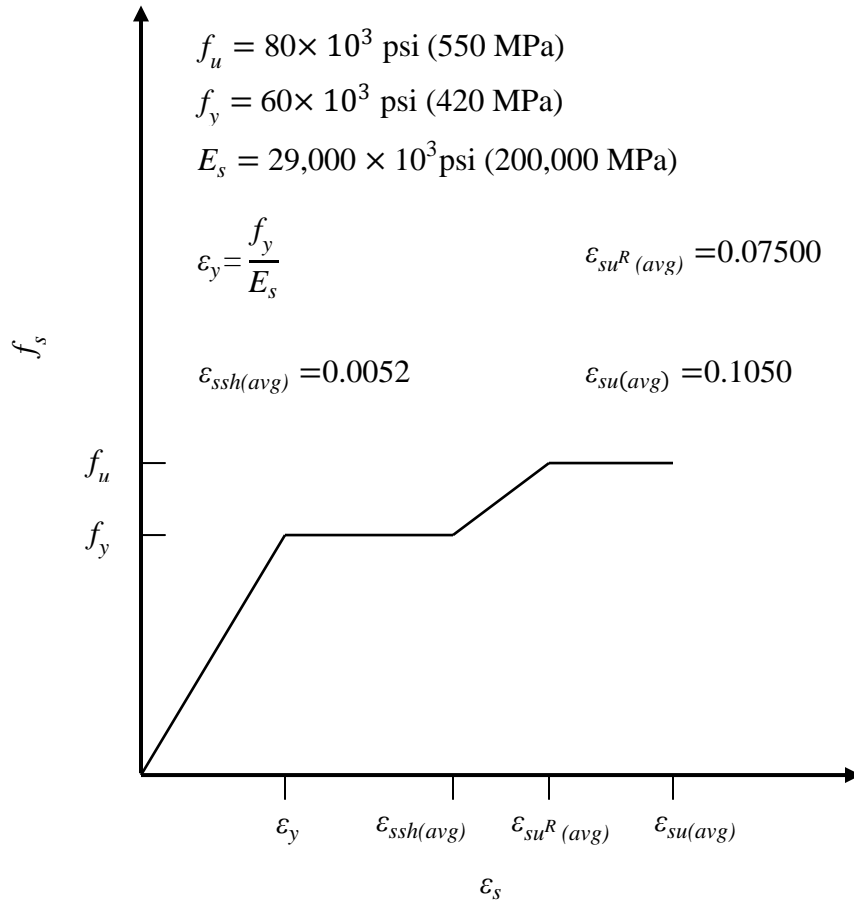


Figure 3.2 Modified CALTRANS stress-strain relationship for Grade 60 steel

Fig.3.2 can be presented by the following equations:

$$f_s = \varepsilon_y E_s \quad 0 \leq \varepsilon_s \leq \varepsilon_y \quad \text{Eq.3.10}$$

$$f_s = f_y \quad \varepsilon_y < \varepsilon_s \leq \varepsilon_{ssh(avg)} \quad \text{Eq.3.11}$$

$$f_s = f_y + \left[\frac{\varepsilon_s - \varepsilon_{ssh(avg)}}{\varepsilon_{su^R(avg)} - \varepsilon_{ssh(avg)}} (f_u - f_y) \right] \quad \varepsilon_{ssh(avg)} < \varepsilon_s \leq \varepsilon_{su^R(avg)} \quad \text{Eq.3.12}$$

$$f_s = f_u \quad \varepsilon_{su^R(avg)} < \varepsilon_s \leq \varepsilon_{su(avg)} \quad \text{Eq.3.13}$$

3.4 Prestressing Steel

In ACI-318-11 section 18.7.2, equation 18.1 is used to determine the stress in the pretensioning strands when it is located in the tension zone. However, post tensioning strands will be used at the concrete compression zone to reduce camber. In that case, ACI 318-11 recommends in R18.7.2 to use the strain compatibility and equilibrium method to determine the stress level in the pretensioning strands. Therefore, the PCI 2011 stress-strain relationship for prestressing steel will be adopted in this study Fig.3.3. The stress-strain relation for the 2 most common types of 7-wire low relaxation prestressing strands can be presented as follows:

- 250 ksi Strand:

For $\varepsilon_{ps} < \varepsilon_{py}$

$$f_{ps} = E_p \varepsilon_{ps} \quad \text{psi} \quad \text{Eq.3.14a}$$

$$f_{ps} = E_p \varepsilon_{ps} \quad \text{MPa} \quad \text{Eq.3.14b}$$

For $\varepsilon_{ps} \geq \varepsilon_{py}$

$$f_{ps} = 250 \times 10^3 - \frac{0.25}{\varepsilon_{ps}} \quad \text{psi} \quad \text{Eq.3.15a}$$

$$f_{ps} = 1725 - \frac{1.72}{\varepsilon_{ps}} \quad \text{MPa} \quad \text{Eq.3.15b}$$

- 270 ksi Strand:

For $\varepsilon_{ps} < \varepsilon_{py}$

$$f_{ps} = E_p \varepsilon_{ps} \quad \text{psi} \quad \text{Eq.3.16a}$$

$$f_{ps} = E_p \varepsilon_{ps} \quad \text{MPa} \quad \text{Eq.3.16b}$$

For $\varepsilon_{ps} \geq \varepsilon_{py}$

$$f_{ps} = 270 \times 10^3 - \frac{0.04}{\varepsilon_{ps} - 0.007} \quad \text{psi} \quad \text{Eq.3.17a}$$

$$f_{ps} = 1860 - \frac{0.276}{\varepsilon_{ps} - 0.007} \quad \text{MPa} \quad \text{Eq.3.17b}$$

ε_{py} is the yield prestressing strain and its equal to 0.0076 for 250 ksi strand and 0.0086 for 270 ksi strand. The modulus of elasticity E_p will be taken as $28,500 \times 10^3$ psi (196,500 MPa).

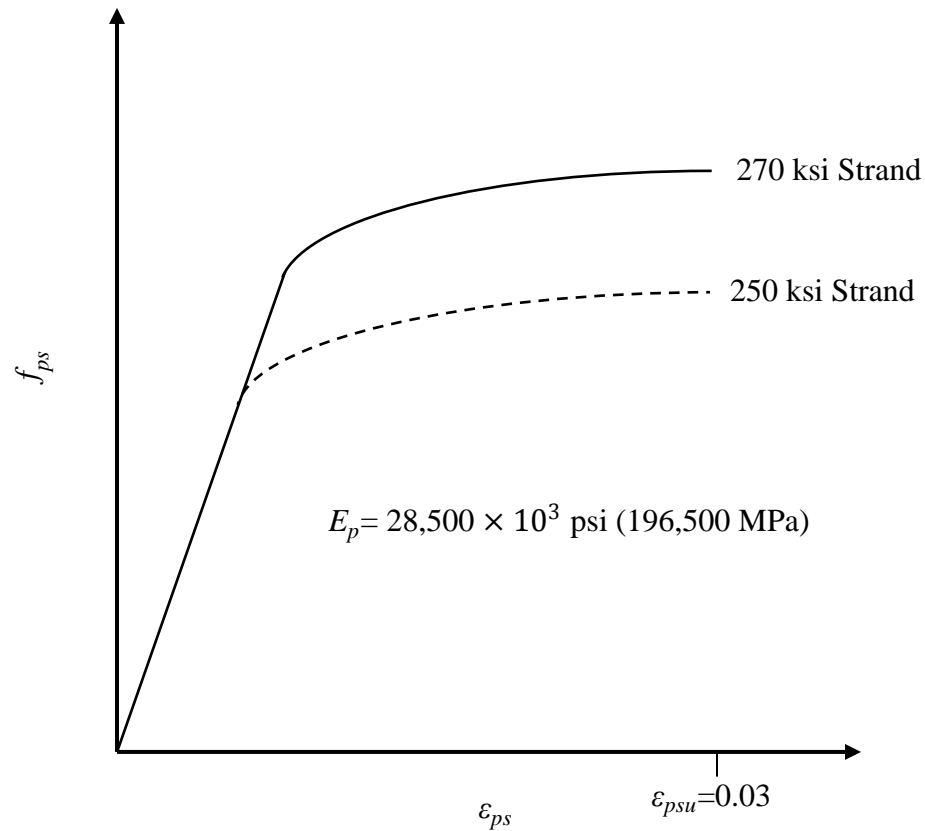


Figure 3.3 Stress-strain relationships of 7-wire low relaxation prestressing steel strands

3.5 Summary

This chapter presented the properties of the materials that prestressed concrete bridge girders are consisted of through introducing the stress-strain relations for these materials. Thus, the modified Hognestad relation will be used to compute stresses in concrete, the modified CALTRANS model is used for mild steel, and the PCI 2011 relations for 7-wire low relaxation is used for the post and prestressed strands.

CHAPTER 4

MOMENT-CURVATURE DIAGRAM OF PRESTRESSED CONCRETE BRIDGE GIRDERS

4.1 Introduction

This chapter presents the method used in this study to evaluate the moment-curvature diagram of prestressed concrete bridge girders based on the material properties presented in chapter 2 and the principles of mechanics. The moment –curvature diagram will be used to study the effect of the post tensioning strands on the bridge girder capacity. For illustrative purposes, this study will include three types of cross sections: PCI-8 I-girder Fig.A.19, AHHTO type-4 girder Fig.A.20, and AASHTO B54x34 box beam Fig.A.21. Numerical results will be presented for the PCI-8 girder.

4.2 Basic Assumptions

The moment- curvature diagram ($M-\phi$) is generated on the basis of the following assumptions:

- A Perfect bond exists between the reinforcements and the concrete
- Plane sections remain plane under bending. Consequently, the strain in the concrete and reinforcement are proportional to the distance from the neutral axis
- The maximum strain in concrete nowhere exceeds 0.003
- The area of concrete displaced by reinforcement will be accounted for

4.3 Prestressed Concrete Bridge Girders Cross Sectional Moment

The moment of a cross section is derived by summing the following moment components: concrete, mild steel, and pre and post tensioning steel. In this section, the (M- ϕ) diagram is derived for a rectangular cross-section to illustrate the process Fig.4.1.

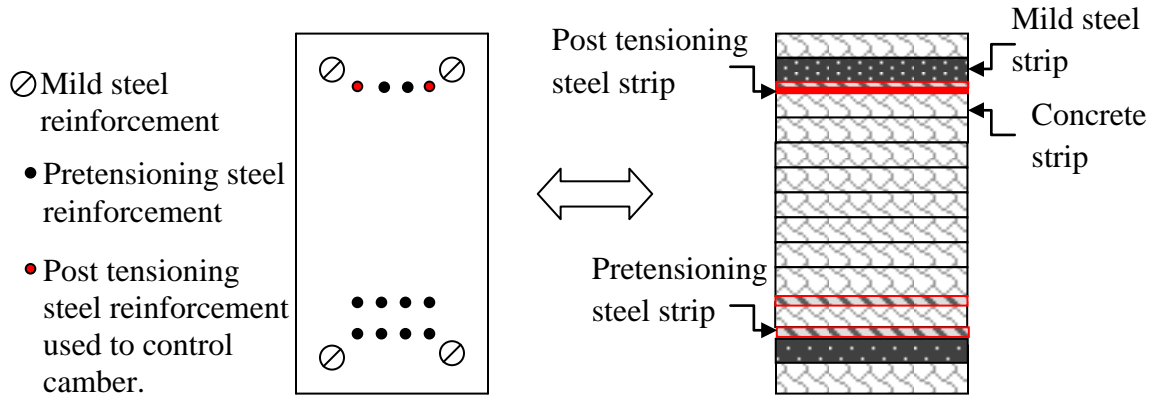


Figure 4.1 Rectangular beam cross section and reinforcement details

4.3.1 Concrete Forces

4.3.1.1 Concrete Compressive Forces

As shown in Fig.4.2, the concrete compression zone of the beam will be divided into N concrete strips and the force will be calculated for each strip. In order to do that, the concrete strain ϵ_{ci} will be computed at the mid-height of each strip i and d_{ci} will represent the distance from the mid-height of strip i to the outermost concrete fiber compression.

$$\epsilon_{ci} = \epsilon_c \left(\frac{kd - d_{ci}}{kd} \right) \quad \text{Eq.4.1}$$

The concrete force C_{ci} in strip i can be calculated as:

$$C_{ci} = f_{ci} b \frac{h}{N} \quad kd \geq h \text{ (when the entire cross-section is in compression)} \quad \text{Eq.4.2a}$$

Or

$$C_{ci} = f_{ci} b \frac{kd}{N} \quad kd < h \text{ (when cross-section is partially in compression)} \quad \text{Eq.4.2b}$$

Where ε_c is the strain in the outermost concrete fiber in compression, and kd is the distance from the neutral axis to the outermost concrete fiber in compression.

The moment of each concrete strip can be presented as follows:

$$M_{cci} = C_{ci} d_{ci} \quad \text{Eq.4.3}$$

$$M_{cc} = \sum_{i=1}^N C_{ci} d_{ci} \quad \text{Eq.4.4}$$

b and h are the width and depth respectively of the rectangular beam cross-section. f_{ci} is the concrete stress for strip i corresponding to strain level ε_{ci} . Eq. 4.2b is used when part of the cross section is in compression (neutral axis is located within the beam cross section or $kd < h$). In order to avoid overestimation of the bridge girder strength, the concrete area displaced by reinforcement should be accounted for. The moment due to the concrete area displaced by reinforcement at the concrete compression zone can be calculated as follows:

$$M_{cr} = \sum_{i=1}^N A_{ri} f_{cri} d_{ri} \quad \text{Eq.4.5}$$

Where:

M_{cr} = moment due to concrete area displaced by reinforcement at the concrete compression zone

N = number of reinforcement layers at the concrete compression zone

A_{ri} = area of reinforcement layer i

f_{cri} = concrete stress at reinforcement layer i Fig.4.2d

d_{ri} = distance from the center of reinforcement layer i to the outermost concrete fiber in compression

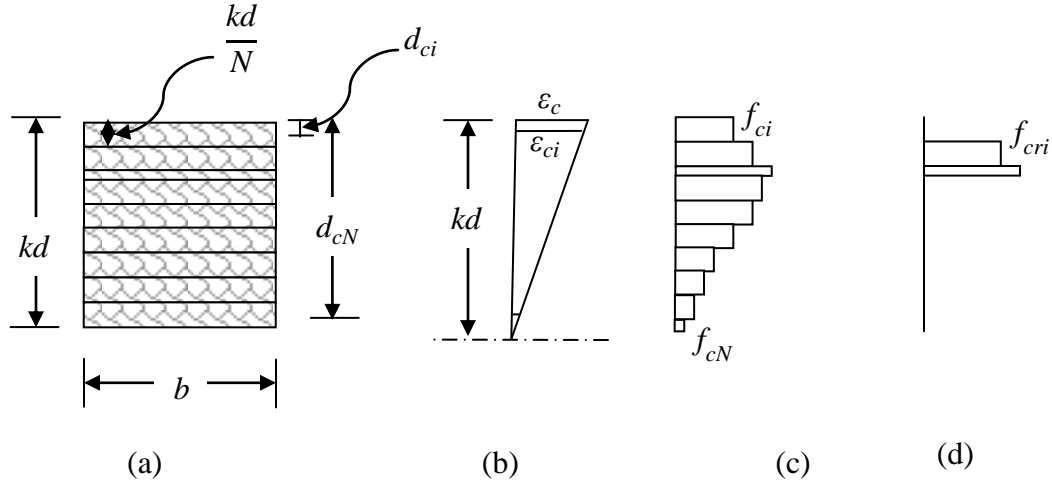


Figure 4.2 (a) Concrete compression side strips, (b) strain distribution, (c) stresses and (d) concrete stresses at reinforcement layers

4.3.1.2 Concrete Tensile Forces

Since this study focuses on the behavior of bridge girders prior to placement in the field, the influence of the concrete tension force can be significant. The contribution of the concrete in the tension zone is accounted for until the strain in the outermost concrete fiber in tension reaches the strain at cracking ε_{cr} .

The concrete tension zone in the beam cross section will be divided into N concrete strips and the force will be calculated for each strip Fig.4.3. In order to do that, the concrete strain ε_{ci} will be computed at the mid-height of each strip i , and d_{ti} will represent the distance from the mid-height of strip i to the outermost concrete fiber in compression.

$$\varepsilon_{ci} = \varepsilon_c \left(\frac{d_{ti} - kd}{kd} \right) \quad \text{Eq.4.6}$$

The concrete force C_{ti} in strip i can be calculated as:

$$C_{ti} = \varepsilon_{ci} b \frac{h - kd}{N} \quad \text{Eq.4.7}$$

Where ε_c is the strain in the outermost concrete fiber in compression, and kd is the distance from the neutral axis to the outermost concrete fiber in compression.

The moment of each concrete strip can be presented as follows:

$$M_{cti} = C_{ti} d_{ti} \quad \text{Eq.4.8}$$

$$M_{ct} = \sum_{i=1}^N C_{ti} d_{ti} \quad \text{Eq.4.9}$$

In order to avoid overestimation of the bridge girder strength, the concrete area displaced by reinforcement should be accounted for. The moment due to the concrete area displaced by reinforcement at the concrete tension zone can be calculated as follows:

$$M_{tr} = \sum_{i=1}^N A_{ri} f_{tri} d_{ri} \quad \text{Eq.4.10}$$

Where:

M_{tr} = moment due to concrete area displaced by reinforcement at the concrete tension zone

N = number of reinforcement layers at the concrete tension zone

A_{ri} = area of reinforcement layer i

f_{tri} = concrete stress at reinforcement layer i Fig.4.3d

d_{ri} = distance from the center of reinforcement layer i to the outermost concrete fiber in compression

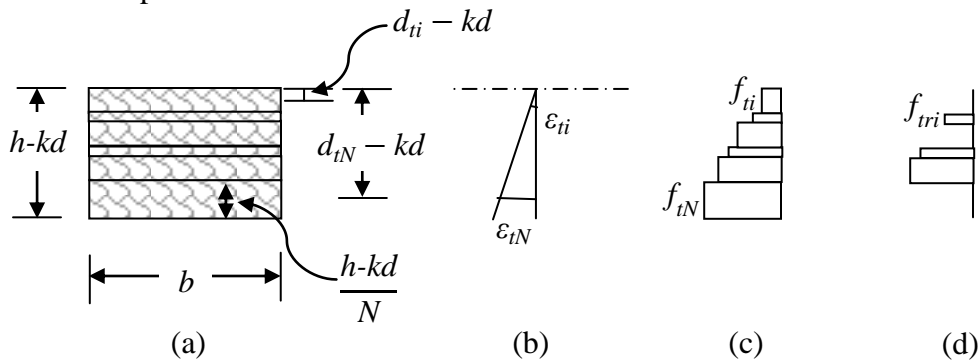


Figure 4.3 (a) Concrete tension side strips, (b) strain distribution, (c) stresses and (d) concrete stresses at reinforcement layers

4.3.2 Mild Steel Reinforcement Forces

For an assumed kd value, the mild reinforcement strain ε_{si} at layer i can be computed as follows:

$$\varepsilon_{si} = \varepsilon_c \left(\frac{kd - d_{si}}{kd} \right) \quad \text{Eq.4.11}$$

d_{si} is measured from the center of the mild steel layer i to the outermost concrete fiber in compression Fig.4.4. Note that when ε_{si} is positive, the mild steel is in compression. Once the strain ε_{si} at the steel layer i is known, the corresponding stress f_{si} can be determined using the stress-strain relationship introduced in chapter 2. The moment for each steel layer can be expressed as:

$$M_{si} = f_{si} A_{si} d_{si} \quad \text{Eq.4.12}$$

$$M_s = \sum_{i=1}^N f_{si} A_{si} d_{si} \quad \text{Eq.4.13}$$

A_{si} is the mild steel area for layer i .

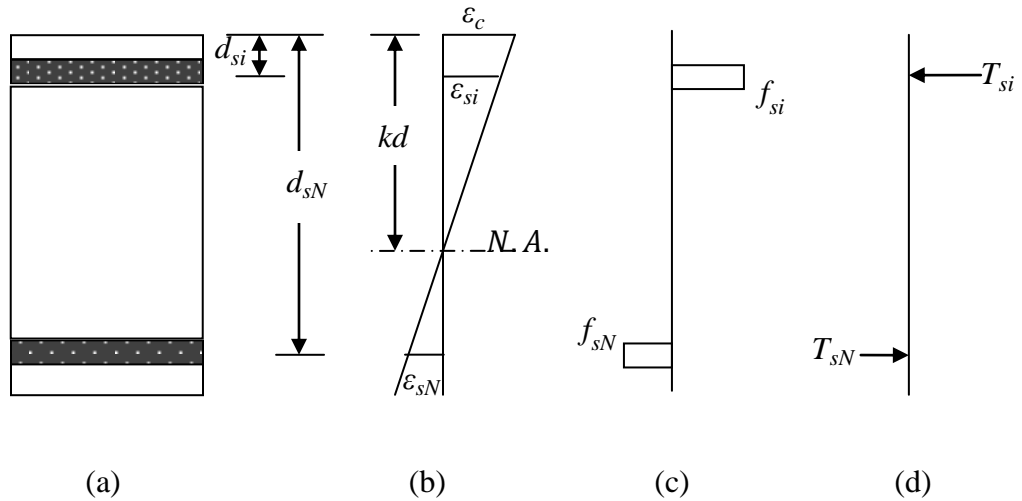


Figure 4.4 (a) Mild steel layouts, (b) strain distribution, (c) stresses and (d) forces

4.3.3 Pretensioning Steel Forces

For an assumed kd value, the flexural pretensioning reinforcement strain ϵ_{psi} at layer i can be computed as follows:

$$\epsilon_{sai} = \epsilon_c \left(\frac{kd - d_{pi}}{kd} \right) \quad \text{Eq.4.14}$$

$$\epsilon_{sei} = \frac{f_{se}}{E_{ps}} \quad \text{Eq.4.15}$$

$$\epsilon_{cei} = \frac{f_{c(c.g.s)i}}{E_c} \quad \text{Eq.4.16}$$

$$\epsilon_{psi} = \epsilon_{sai} + \epsilon_{sei} + \epsilon_{cei} \quad \text{Eq.4.17}$$

From Eq.4.17, the total strain in each pretensioning steel layer is the sum of three portions: the compressive strain ϵ_{cei} in concrete at the prestressing steel layer i due to effective prestress only, ϵ_{sei} which is the strain in prestressing layer i due to effective prestress only, and ϵ_{sai} is the increase in strain in prestressing layer i at a specific concrete strain level ϵ_c . d_{pi} is measured from the center of prestressing layer i to the outermost concrete fiber in compression Fig.4.5. Once ϵ_{psi} is known, the pretensioning stress f_{psi} can be calculated using stress strain relationships presented in chapter 2.

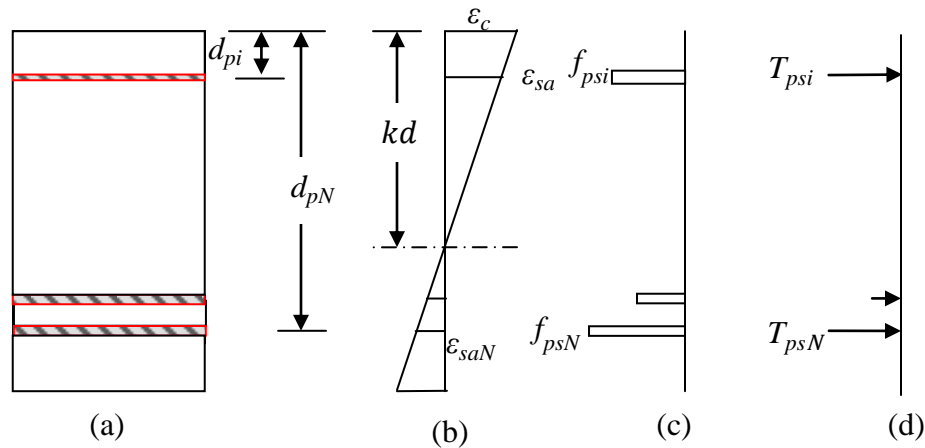


Figure 4.5 (a) Pretensioning steel layout, (b) strain distribution, (c) stresses and (d) forces

The effective prestress f_{se} can be determined as follows:

$$f_{se} = f_{pj} - \Delta f_s \quad \text{Eq.4.18}$$

Δf_s is the total losses in pretensioning strands from time of release to prior placement in sub structure. The jacking prestress should be within the limits specified by ACI 318-11 section 2 and 10.8.3. Eq.4.19 and Eq.4-20 present the jacking stress limits:

- For pretensioning strands:

$$f_{pj} \leq 0.94f_{py} \text{ and } f_{pj} \leq 0.80f_{pu} \quad \text{Eq.4.19}$$

- For post tensioning strands:

$$f_{pj} \leq 0.70f_{pu} \quad \text{Eq.4.20}$$

The moment due to pretensioning steel layer i can be represented as:

$$M_{pi} = f_{psi} A_{psi} d_{pi} \quad \text{Eq.4.21}$$

$$M_p = \sum_{i=1}^N f_{psi} A_{psi} d_{pi} \quad \text{Eq.4.22}$$

Where A_{psi} is the area of pretensioning steel layer i .

4.3.4 Post Tensioning Steel Used to Control Camber

For an assumed kd value, the post tensioning reinforcement strain ϵ'_{psi} used to control camber at layer i can be computed as follows:

$$\epsilon'_{sai} = \epsilon_c \left(\frac{kd - d'_{pi}}{kd} \right) \quad \text{Eq.4.23}$$

$$\epsilon'_{sei} = \frac{f'_{se}}{E_{ps}} \quad \text{Eq.4.24}$$

$$\epsilon'_{cei} = \frac{f_{c(c.g.s)i}}{E_c} \quad \text{Eq.4.25}$$

$$\epsilon'_{psi} = \epsilon'_{sai} + \epsilon'_{sei} + \epsilon'_{cei} \quad \text{Eq.4.26}$$

The total strain in each post tensioning steel layer is the sum of three portions which are the compressive strain in concrete ϵ'_{se} at the post tensioning steel layer due to effective prestress only, the effective prestressing strain ϵ'_{se} and the increase in strain ϵ'_{sa} at a specific strain concrete level ϵ_c . Once ϵ'_{psi} is known, the post tensioning stress f'_{psi} can be calculated using stress strain relationships presented in chapter 2.

d'_p is measured from the center post tensioning steel to the extreme compression fiber of concrete Fig.4.5. f'_{se} is the effective post stress which can be determined as follows:

$$f'_{se} = f'_{pj} - \Delta f_s \quad \text{Eq.4.27}$$

The jacking post stress f'_{pj} should be within the limits specified by ACI 318-11 which are presented in Eq.4.19 and Eq.4.20. The moment due to post tensioning steel layer A'_{psi} used to control camber can be represented as:

$$M'_{pi} = f'_{psi} A'_{psi} d'_{pi} \quad \text{Eq.4.28}$$

$$M_p = \sum_{i=1}^N f'_{psi} A'_{psi} d'_{pi} \quad \text{Eq.4.29}$$

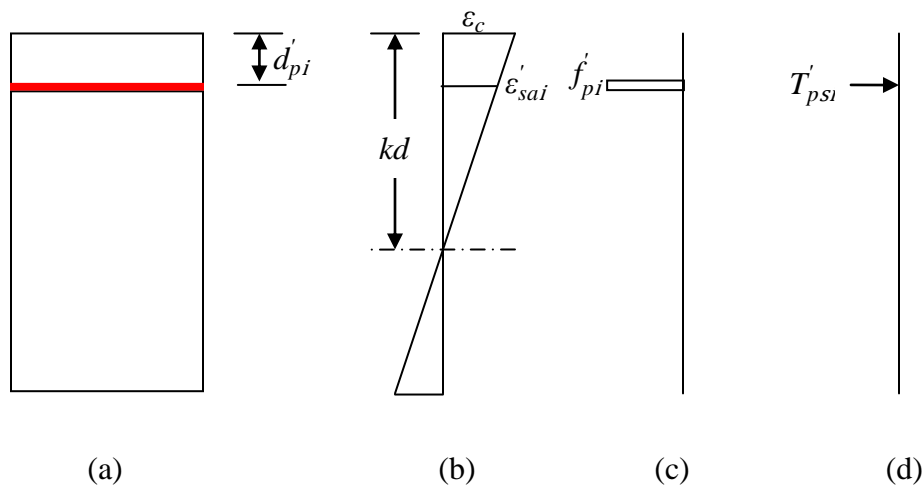


Figure 4.6 (a) Post tensioning steel layout, (b) strain distribution, (c) stresses and (d) forces

4.3.5 Moment -Curvature (M- ϕ)

The cross sectional moment of a prestressed concrete beam is defined by summing the moments of its components and can be expressed as follows:

$$M = (M_{cc} - M_{ccr}) + (M_{ct} - M_{ctr}) + M_s + M_p + M_p' \quad \text{Eq.4.30}$$

The curvature resulting due to a specific strain level ε_c can be computed as follows:

$$\phi = \frac{\varepsilon_c}{kd} \quad \text{Eq.4.31}$$

In order to compute the moment of a beam cross section at a specific strain level, a repeated process will be performed to assume the location of kd . Generating the moment-curvature diagram requires performing a series of computations (i.e. Eq.4.1 to Eq.4.31) to a different magnitude of concrete strain level ε_c . This study will consider a bilinear ($M-\phi$) relationship by considering three points of interest: self-weight point, cracking moment point, and the nominal moment point. The moment-curvature diagram Fig. 4.7 for the PCI-8 girder has been generated based on the assumptions and equations presented in this chapter.

4.4 Summary

Moment- curvature relationships of prestressed concrete bridge girders were based on equilibrium conditions, strain compatibility, material constitutive laws, and assumptions pertinent to prestressed reinforced concrete bridge girders. These relationships will be used in chapter 5 to calculate the camber and camber adjustment, and to evaluate the effect of the post tensioning jacking force on the strength capacity of the bridge girder.

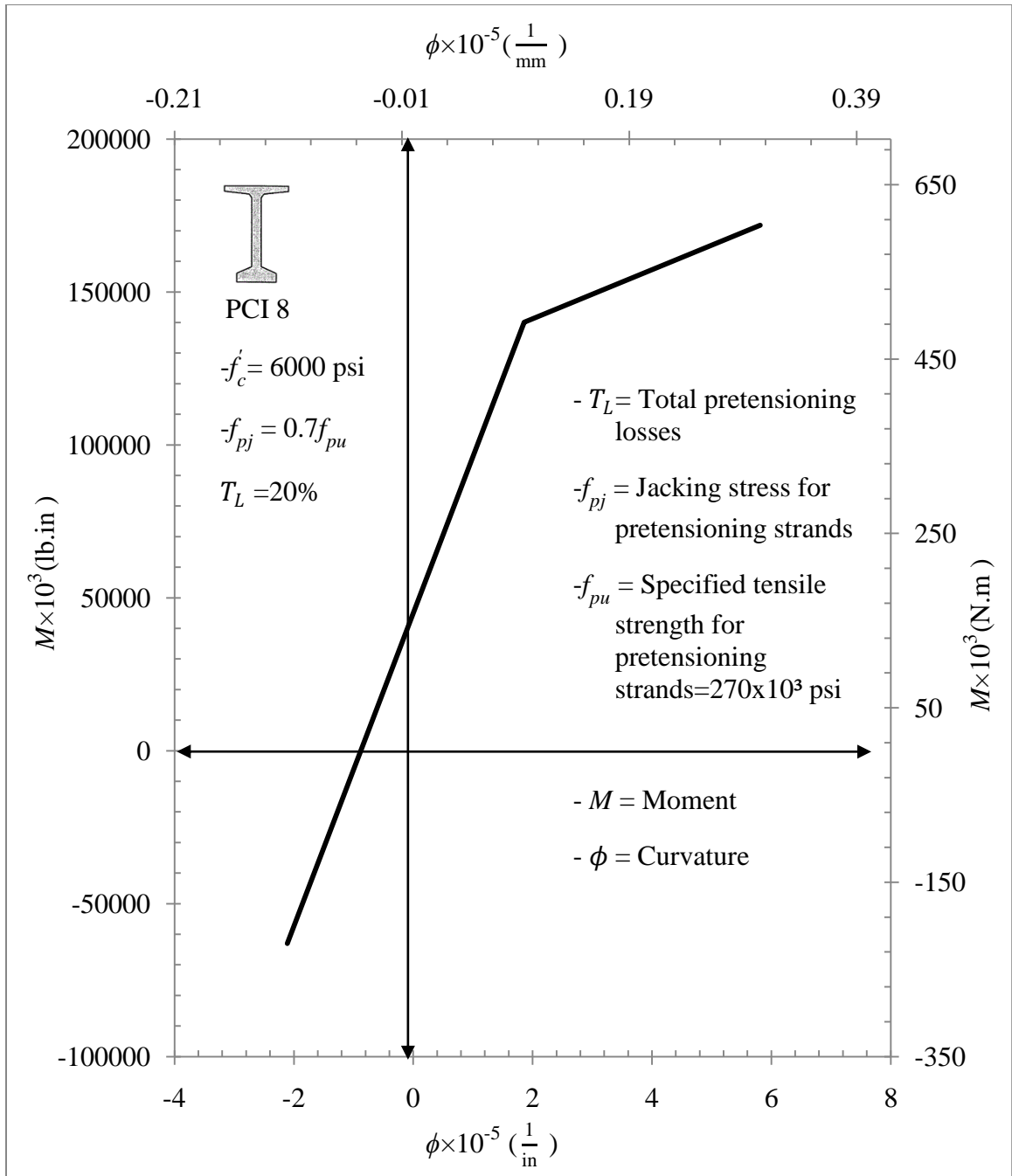


Fig.4.7a Bilinear Moment-Curvature, $M-\phi$, interaction diagram for the PCI-8 girder

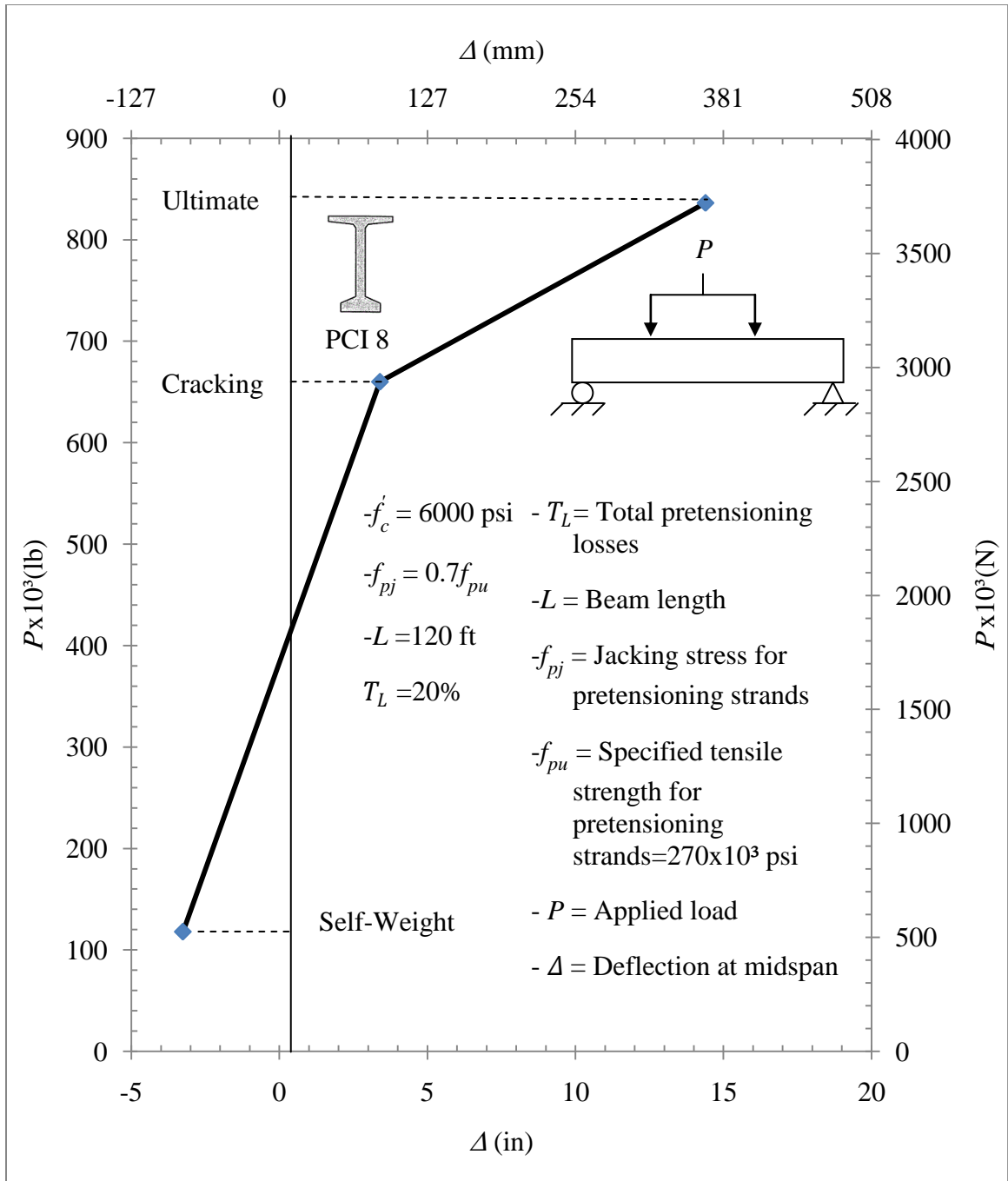


Fig.4.7b Bilinear Load-Deflection, $P-\Delta$, diagram for the PCI-8 girder

CHAPTER 5

CAMBER CONTROL

5.1 Introduction

This chapter presents the Initial camber results obtained from the study and the design camber due to the post tensioning jacking force.

5.2 Basic Assumptions

Camber computations will be based on the following assumptions:

- The maximum concrete tensile strain does not exceed strain at cracking ϵ_{cr} at the stage prior to the deck placement
- Shear deformation is neglected
- The pretensioning strands profile for the PCI-8 girder and AASHTO type-4 girder has double depression points. However, the AASHTO B54x48 box beam has a straight pretensioning strands profile

5.3 Initial Camber

Initial camber is the resultant of summing the upward deflection caused by the effective pretensioning force P_e and the downward deflection due to the beam self weight Δ_{beam} . For illustrative purposes, the rectangular section is used to calculate the initial camber Fig.5.1.

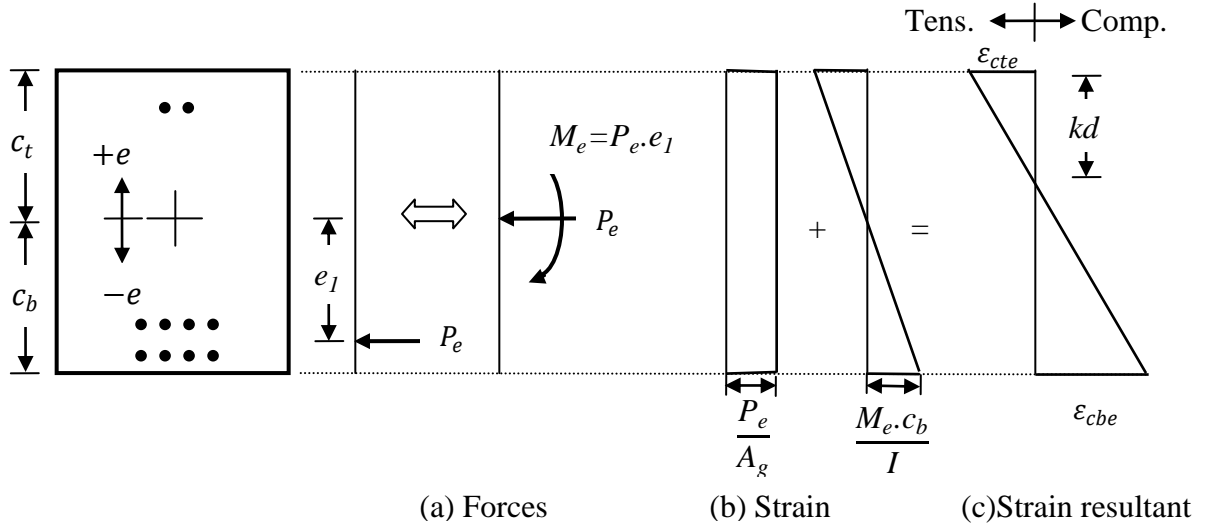


Figure 5.1 (a) Forces and (b) strain distributions in rectangular concrete beam due to effective prestensioning force only

$$\varepsilon_{cte} = \frac{\left(\frac{P_e}{A_g} - \frac{M_e \cdot c_t}{I}\right)}{E_c} \quad \text{Eq.5.1}$$

$$\varepsilon_{cbe} = \frac{\left(\frac{P_e}{A_g} + \frac{M_e \cdot c_b}{I}\right)}{E_c} \quad \text{Eq.5.2}$$

ε_{cte} is the concrete strain at the top outermost fiber and ε_{cbe} is the concrete strain at the bottom outermost fiber due to effective prestress force P_e . A_g is the gross sectional area of the beam. I is the moment of inertia of the cross section. Knowing both the strain at top and the bottom of the beam enables calculating the position of the neutral axis kd

Eq.5.3.

$$kd = \frac{\varepsilon_{cte}}{\varepsilon_{cte} + \varepsilon_{cbe}} h \quad \text{Eq.5.3}$$

$$\phi = \frac{\varepsilon_{cte}}{kd} \quad \text{Eq.5.4}$$

$$\Delta_i = \left[\phi_c \frac{L^2}{8} + (\phi_0 - \phi_c) \frac{a^2}{6} \right] - \Delta_{beam} \quad \text{Eq.5.5}$$

Where:

Δ_i = Initial camber due to effective pretensioning force

ϕ = Curvature

ϕ_c = Curvature at midspan

ϕ_0 = Curvature at support

L = Beam length

a = Distance from end of the beam to the depression point Fig.5.2a

Δ_{beam} = Deflection due to beam self-weight Eq. 5.6

$$\Delta_{beam} = \frac{5wL^4}{384E_cI} \quad \text{Eq.5.6}$$

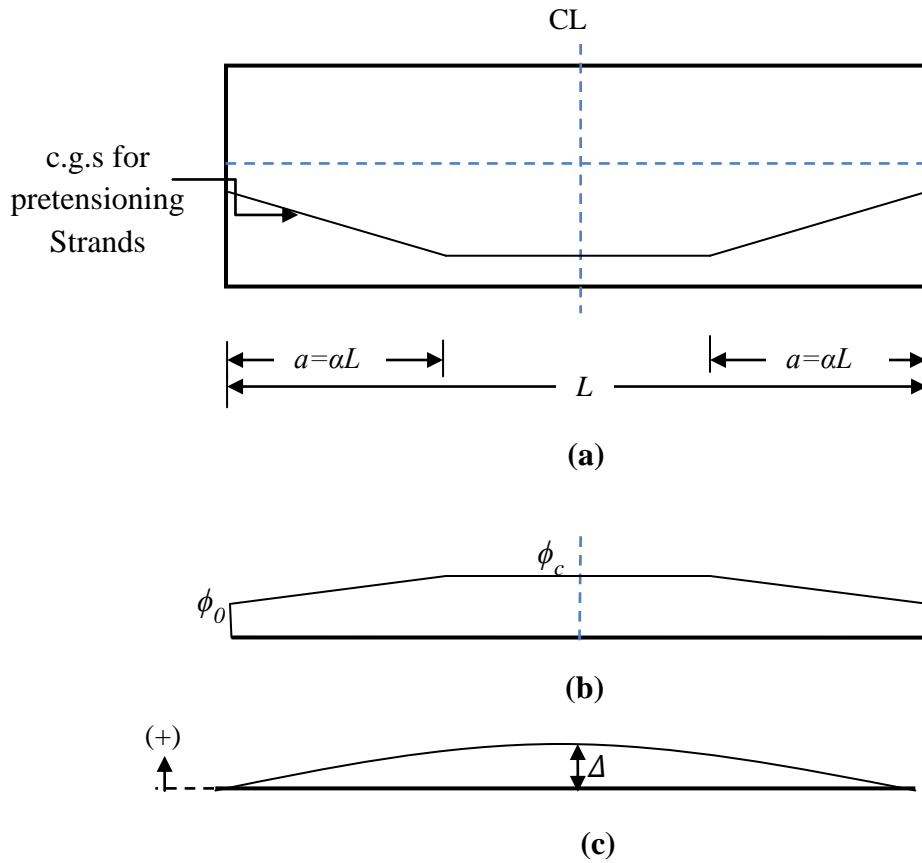


Figure 5.2 (a) Prestressed beam pretensioning strand profile,(b) curvature, and (c) elastic curve for singly supported bridge girder with double

5.4 Design Camber

The design camber is calculated by summing three components: upward deflection due to effective pretensioning force, downward deflection due to bridge girder self-weight, and downward deflection due to post-tensioning jacking force Fig.5.3.

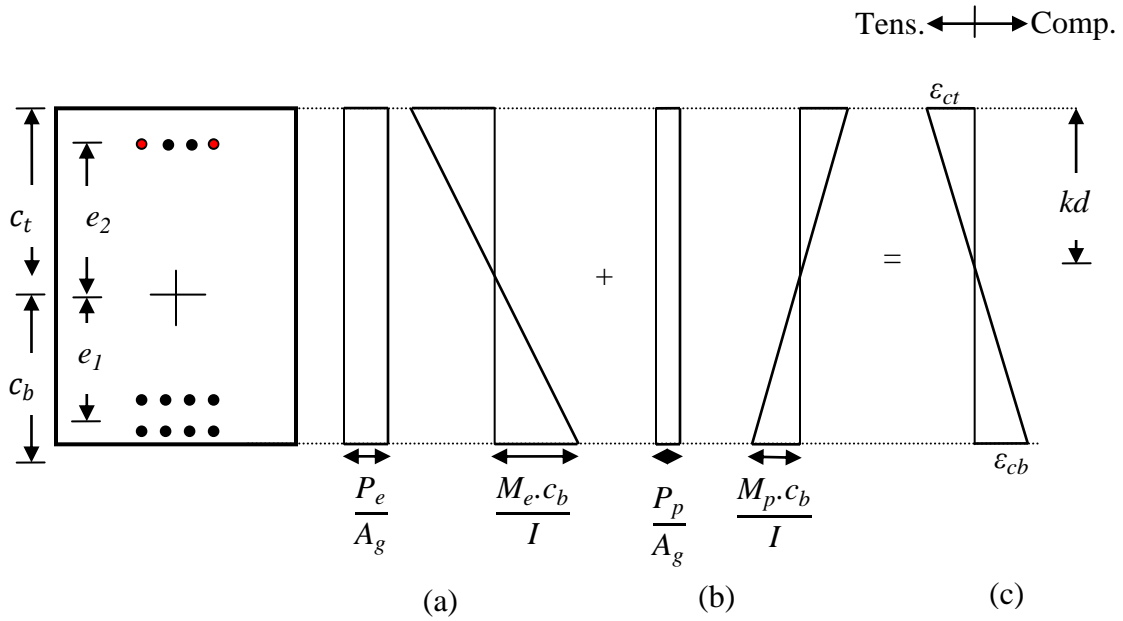


Figure 5.3 (c) Strain distributions in rectangular concrete beam due to (a) effective pretensioning force, P_e and (b) post tensioning force, P_p

$$\epsilon_{ct} = \frac{\left[\frac{(P_e + P_p)}{A_g} - \frac{M_e \cdot c_t}{I} + \frac{M_p \cdot c_t}{I} \right]}{E_c} \quad \text{Eq.5.7}$$

$$\epsilon_{cb} = \frac{\left[\frac{(P_e + P_p)}{A_g} + \frac{M_e \cdot c_b}{I} - \frac{M_p \cdot c_b}{I} \right]}{E_c} \quad \text{Eq.5.8}$$

$$kd = \frac{\epsilon_{ct}}{\epsilon_{ct} + \epsilon_{cb}} h \quad \text{Eq.5.9}$$

$$\phi = \frac{\epsilon_{ct}}{kd} \quad \text{Eq.5.11}$$

$$\Delta_d = \left[\phi_c \frac{L^2}{8} + (\phi_0 - \phi_c) \frac{a^2}{6} \right] - \Delta_{beam} \quad \text{Eq.5.12}$$

Δ_d is the camber after applying the post tensioning force. It should be stressed that this study considers reducing the camber as long as the concrete is not cracked. Relationships between design camber and post tensioning jacking forces Figs. 5.4 – 5.7 have been generated for the PCI-8 girder based on assumptions and equations presented in this chapter. The cross section and its properties are presented in the accompanying figures.

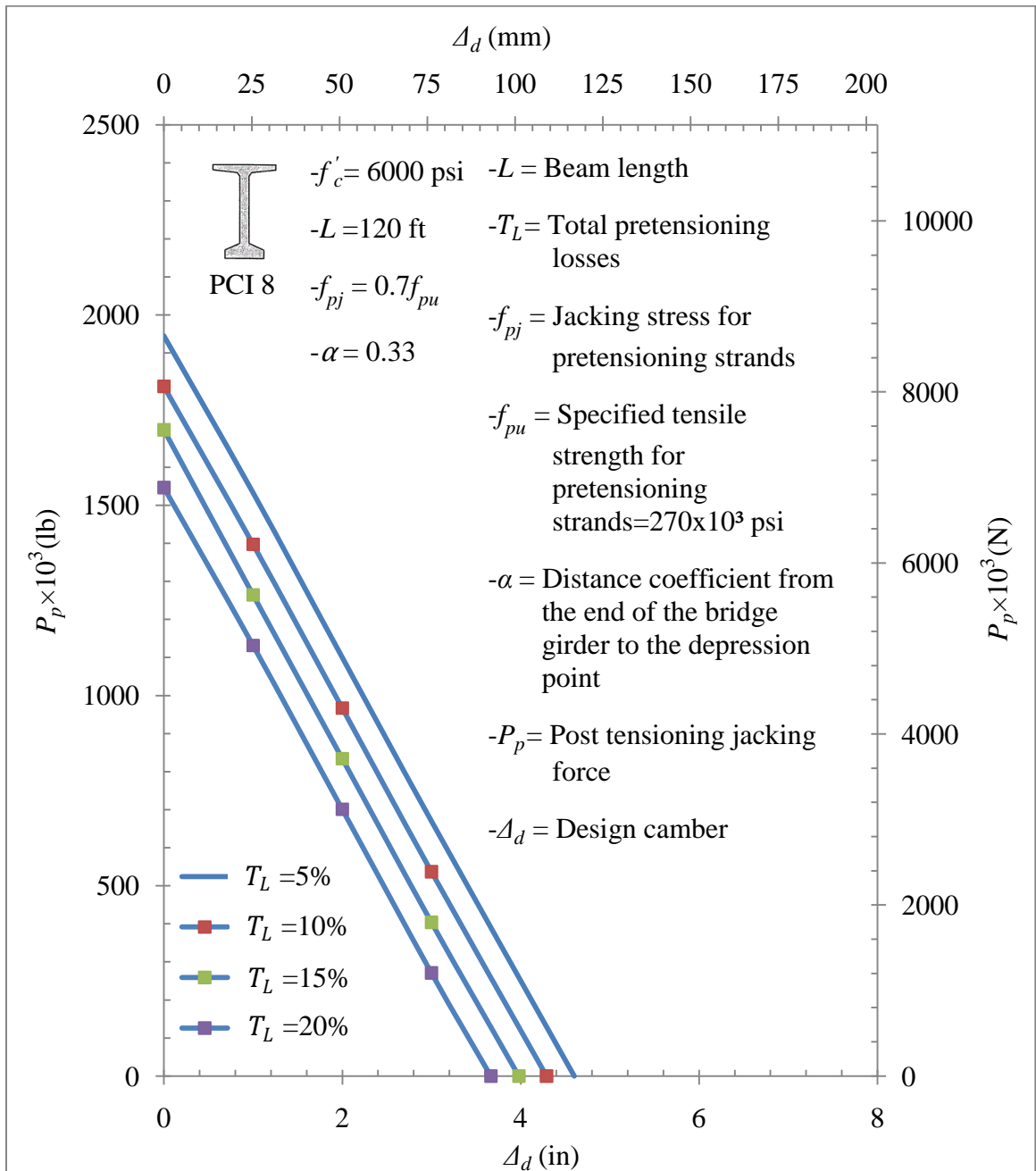


Figure 5.4 Variation of post tensioning Jacking force, P_p , with design camber, Δ_d , for different pretensioning losses, T_L , for the PCI-8 girder

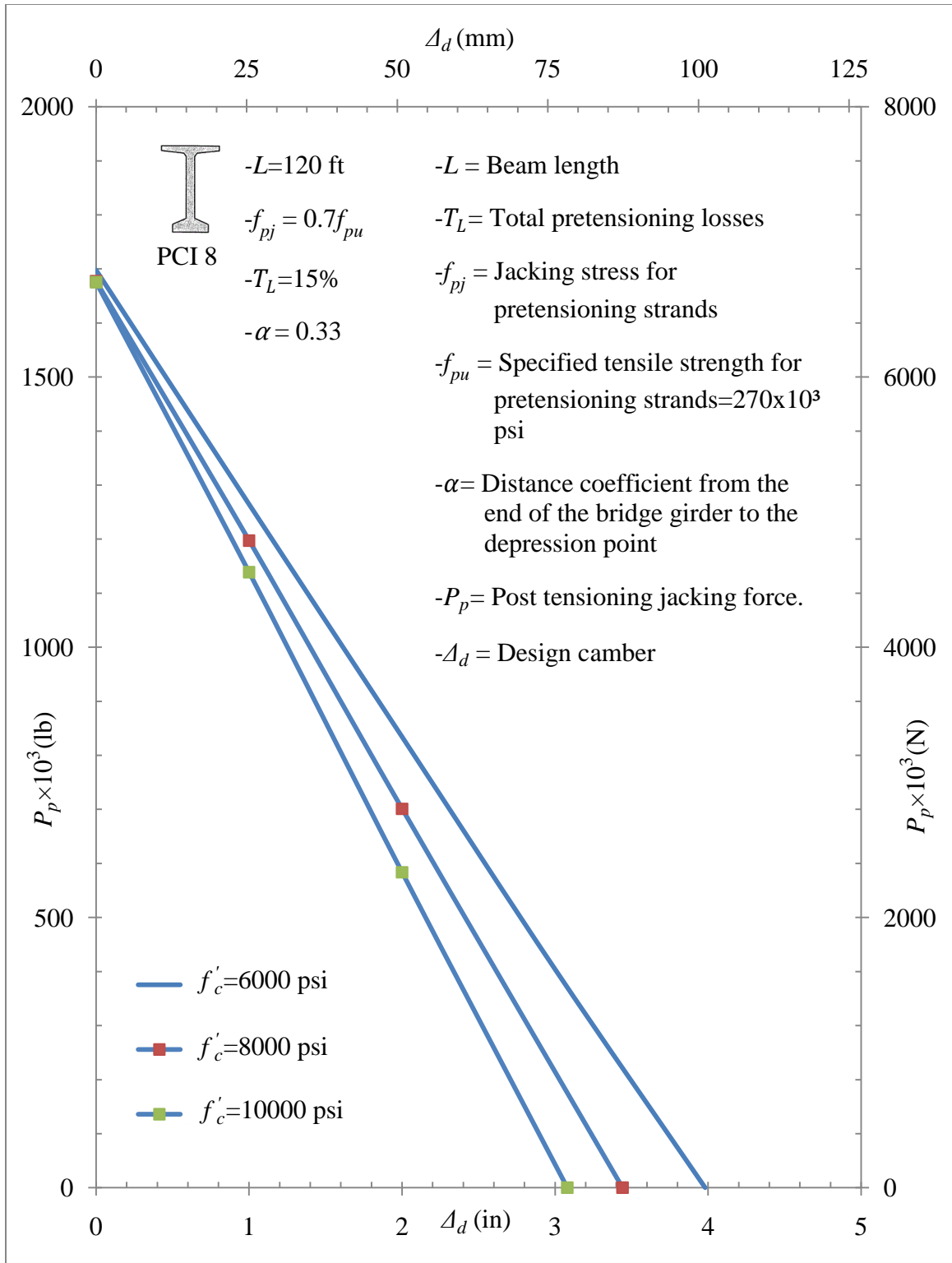


Figure 5.5 Post tensioning Jacking force, P_p , vs. design camber, Δ_d , for different specified concrete strength, f'_c , for the PCI-8 girder

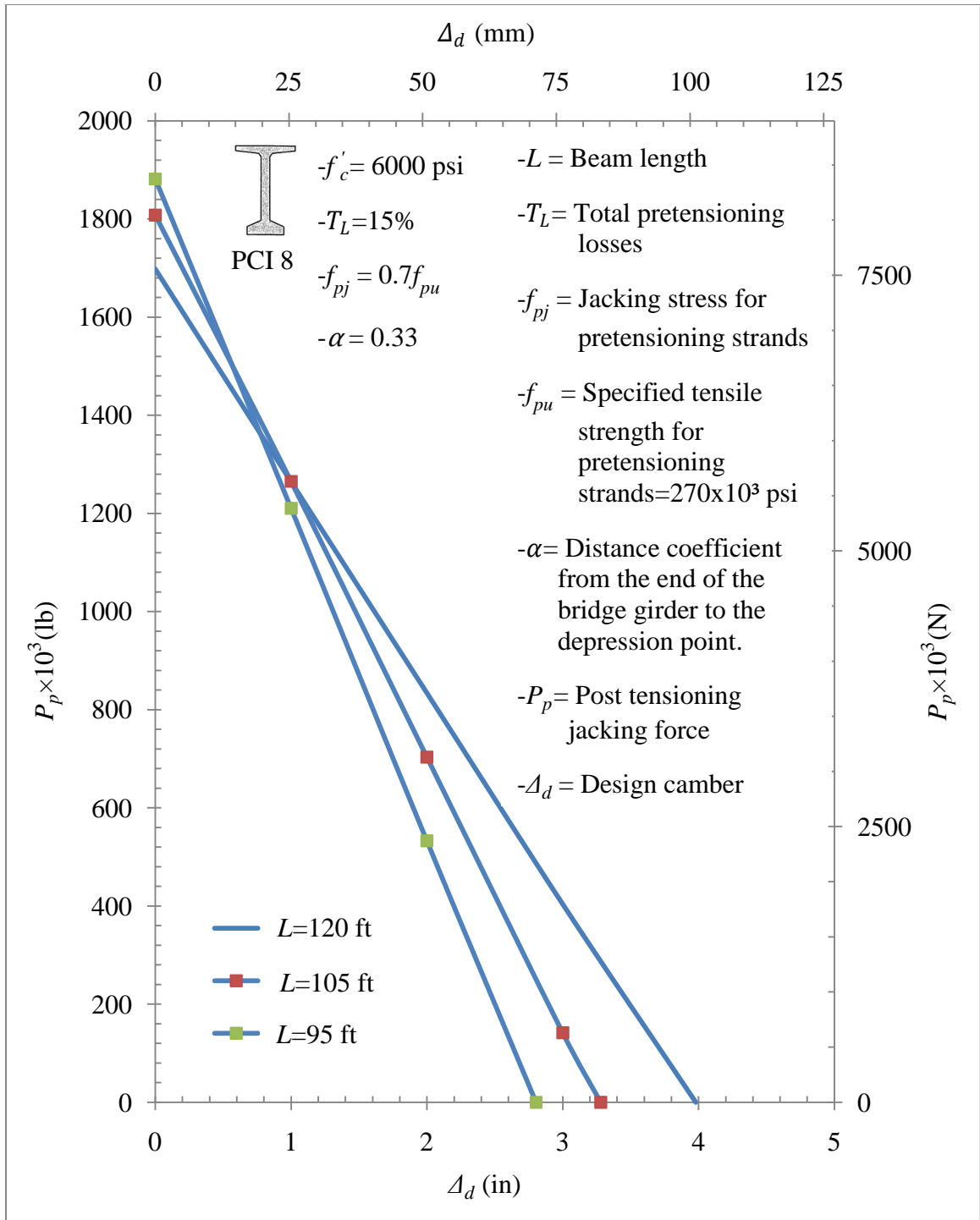


Figure 5.6 Post tensioning Jacking force, P_p , vs. design camber, Δ_d , for different bridge girder length, L , for the PCI-8 girder

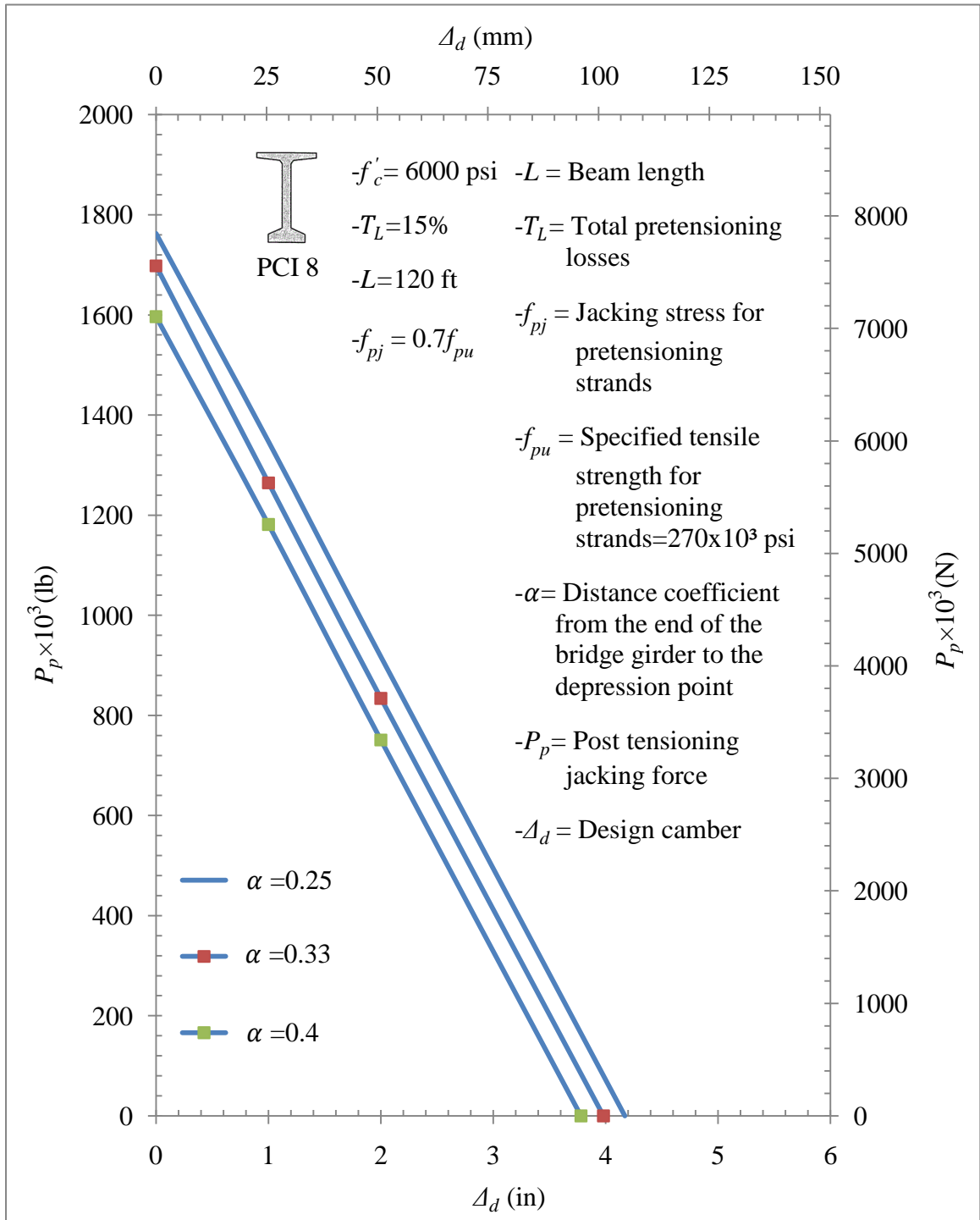


Figure 5.7 Variation of post tensioning Jacking force, P_p , with design camber, Δ_d , with different distance coefficient, α , for the PCI-8 girder

Fig.5.4 -5.7 present the following findings:

- The post tensioning jacking force varies linearly with the design camber which means materials are still in the linear behavior region
- The PCI-8 girder tends to have higher camber with higher specified concrete compression strength
- Using a higher distance coefficient α required higher post tensioning jacking force to produce the same design camber

Relationships between the post tensioning jacking stress and the design camber are derived for the AASHTO type -4 girder and AASHTO B54x48 box beam which are presented in Fig. A-1, A-7.

Using the data obtained from this study enabled generating a general formula for the PCI-8 girder to represent the required post tensioning jacking stress to reduce the camber to be equal to the design camber. This formula is presented in Eq.5.12a, b, and c.

- For $L=120$ ft

$$P_p = 2443 - 1097\alpha - 26.5T_L - A_d(243.67 + 0.0303f'_c) \geq 0 \quad \text{Eq.5.12a}$$

- For $L=105$ ft

$$P_p = 2568 - 1098\alpha - 26.5T_L - A_d(317.33 + 0.0395f'_c) \geq 0 \quad \text{Eq.5.12b}$$

- For $L=95$ ft

$$P_p = 2639 - 1089\alpha - 26.5T_L - A_d(385.33 + 0.0483f'_c) \geq 0 \quad \text{Eq.5.12c}$$

Similar formulas were derived for both the AASHTO type-4 girder and AASHTO B54x48 box beam. These formulas are presented in Eq.5.13a, b, and c and Eq.5.14.a, b, and c.

- For AASHTO Type-4 girder:

- For $L=120$ ft

$$P_p = 1023.2 - 662.7\alpha - 13.5T_L - \Delta_d(94.167 + 0.0119f'_c) \geq 0 \quad \text{Eq.5.13a}$$

$$P_p = 1159.5 - 708\alpha - 13.5T_L - \Delta_d(123.13 + 0.0155f'_c) \geq 0 \quad \text{Eq.5.13b}$$

- For $L=95$ ft

$$P_p = 1220 - 663.3\alpha - 13.5T_L - \Delta_d(149.85 + 0.019f'_c) \geq 0 \quad \text{Eq.5.13c}$$

- For AASHTO B58x48 box beam:

- For $L=120$ ft

$$P_p = 430 - 11.25T_L - \Delta_d(144.92 + 0.0163f'_c) \geq 0 \quad \text{Eq.5.14a}$$

- For $L=105$ ft

$$P_p = 587.8 - 11.25T_L - \Delta_d(189 + 0.0215f'_c) \geq 0 \quad \text{Eq.5.14b}$$

- For $L=95$ ft

$$P_p = 680.83 - 11.25T_L - \Delta_d(225.5 + 0.027f'_c) \geq 0 \quad \text{Eq.5.14c}$$

Where:

P_p = Post tensioning jacking force (kips)

α = Distance coefficient from the end of the bridge girder to the depression point

T_L = Total pretensioning losses from time of release to placement in field Fig.5.2a

Δ_d = Design camber (in)

f'_c = Specified concrete compression strength (psi)

Fig.5.8-5.11 show a comparison between results obtained from Eq.5.12a, b, and c and results obtained from study.

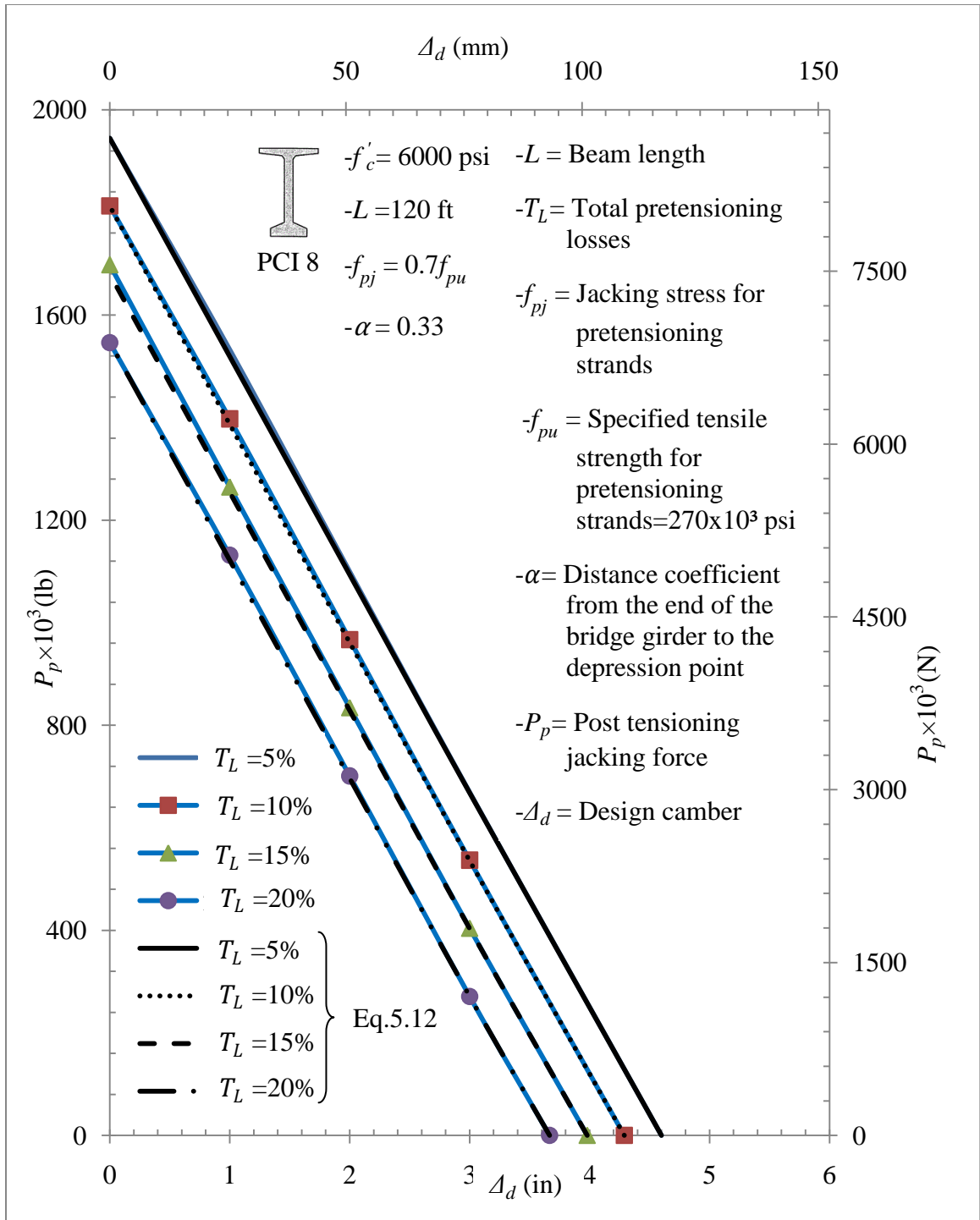


Figure 5.8 Comparison between results obtained from the study and Eq.5-12 for different pretensioning losses, T_L , for the PCI-8 girder

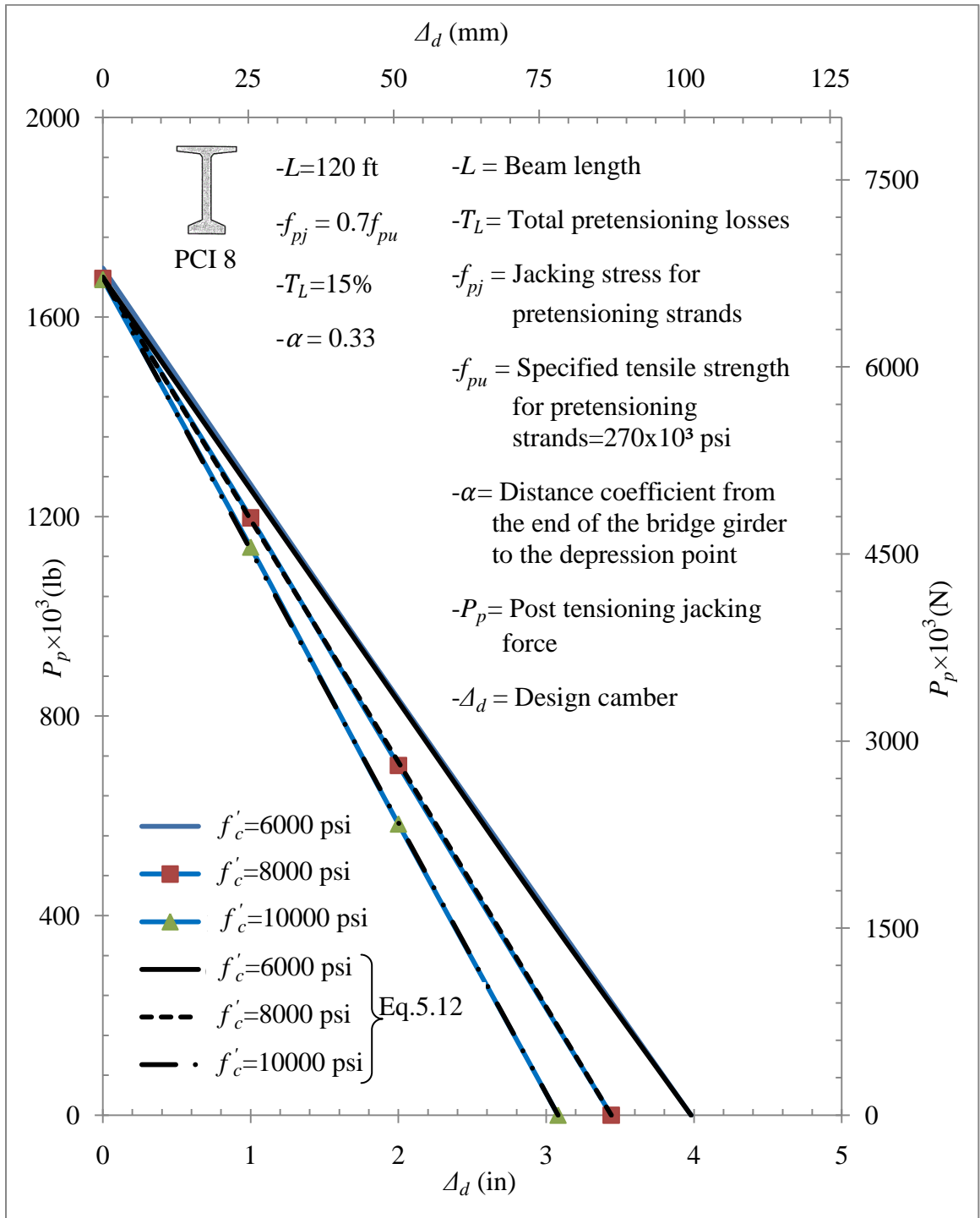


Figure 5.9 Comparison between results obtained from the study and Eq.5-12 for different specified concrete compressive strength, f'_c , for the PCI-8 girder

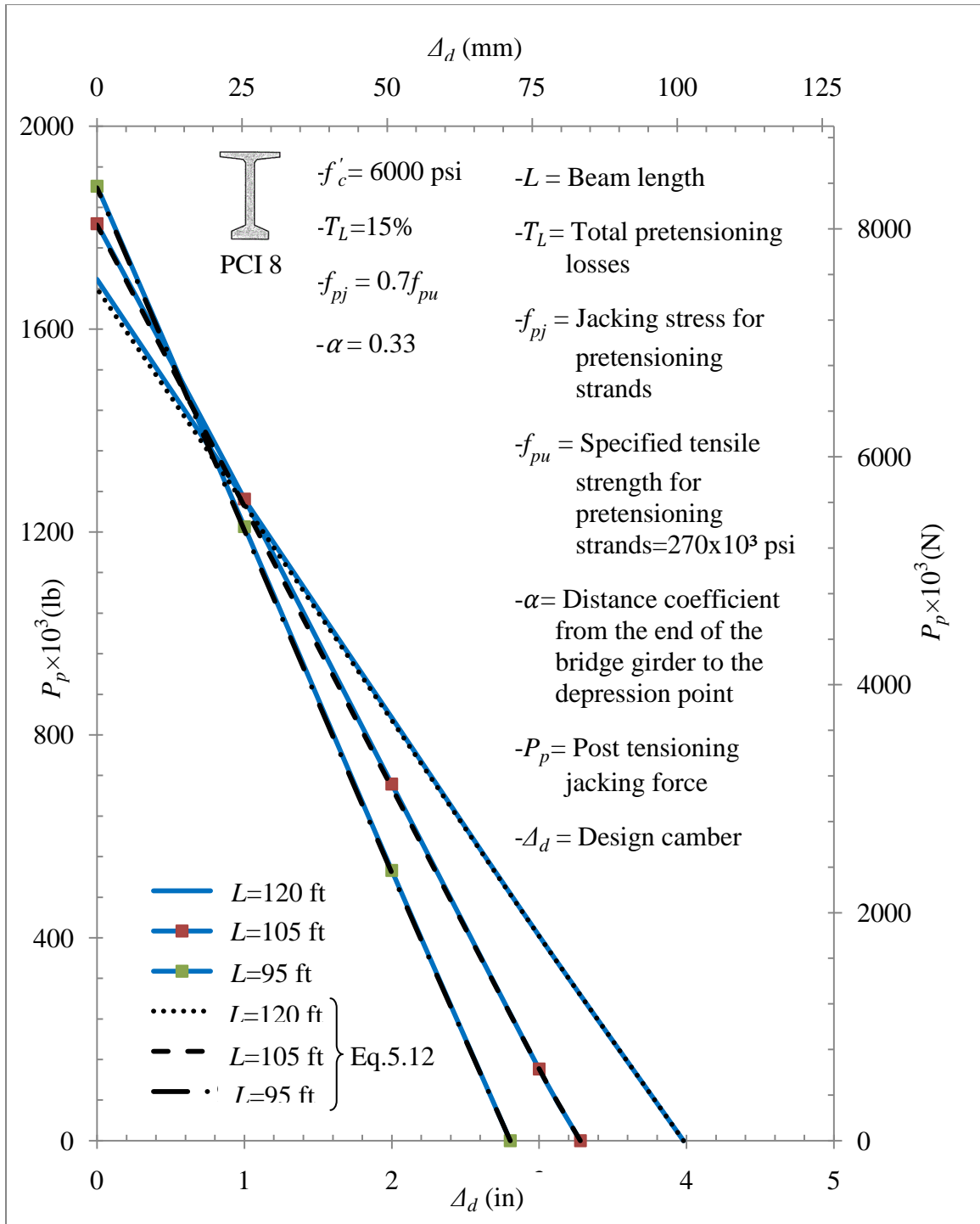


Figure 5.10 Comparison between results obtained from the study and Eq.5-12 for different bridge girder length, L , for the PCI-8 girder

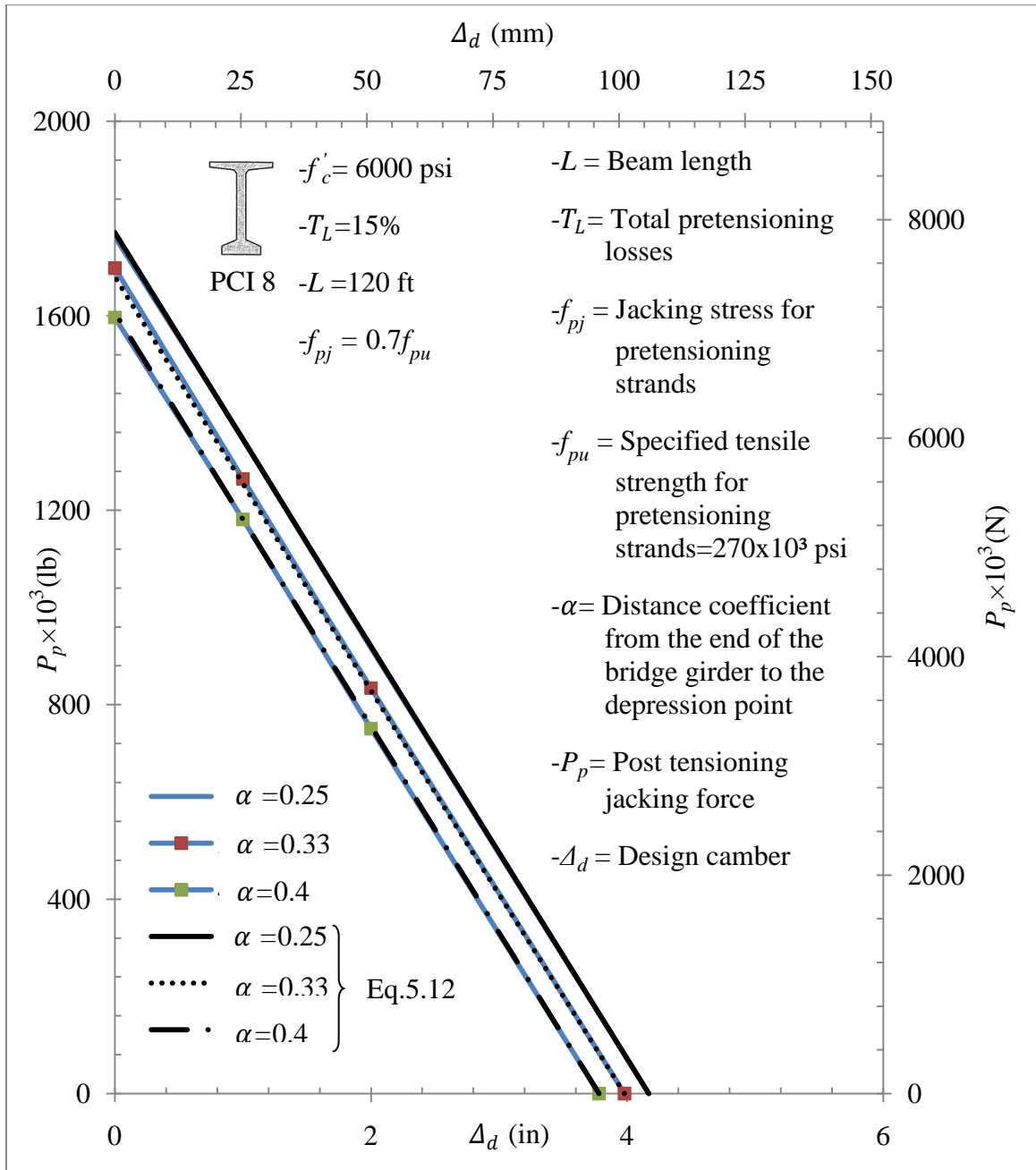


Figure 5.11 Compression between results obtain from the study and from Eq.5.12 with different distance coefficient, α , for the PCI-8 girder

5.5 Example

The PCI8 bridge girder will be used to illustrate how to use the tables and equations to calculate the required post tensioning jacking force to reduce camber. Material properties and dimensions for the bridge girder are listed below:

$$-f'_c = 6000 \text{ psi}$$

$$-T_L = 15\%$$

$$-L = 120 \text{ ft}$$

$$-f_{pj} = 0.7f_{pu}$$

$$-\alpha = 0.33$$

$$-\text{Slab thickness} = 8 \text{ in}$$

$$-\text{Slab width} = 11 \text{ ft}$$

$$\Delta_d = \frac{5w_{slab}L^4}{384E_cI_{girder}} = 1.9 \text{ in}$$

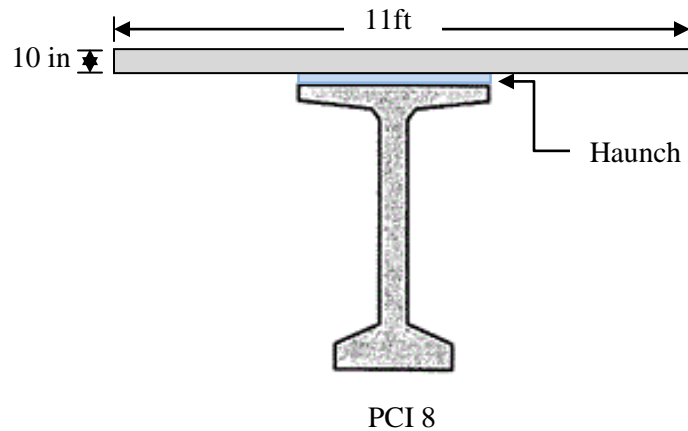


Figure 5.12 Example details

Assuming that the actual camber is 2.5 in, the post tensioning jacking force required reducing camber by (2.5-1.9=0.6 in) is calculated as follows:

1- Calculate P_{p1} that coincide with $\Delta_d = 2.5$ in

2- Calculate P_{p2} that coincide with $\Delta_d = 1.9$ in

3- The required post tensioning jacking force is the difference between P_{p1} and P_{p2}

From Fig.1,

$$P_{p1} = 615 \times 10^3 \text{ lb}$$

$$P_{p2} = 875 \times 10^3 \text{ lb}$$

$$P_p = 880 - 615 = 260 \times 10^3 \text{ lb}$$

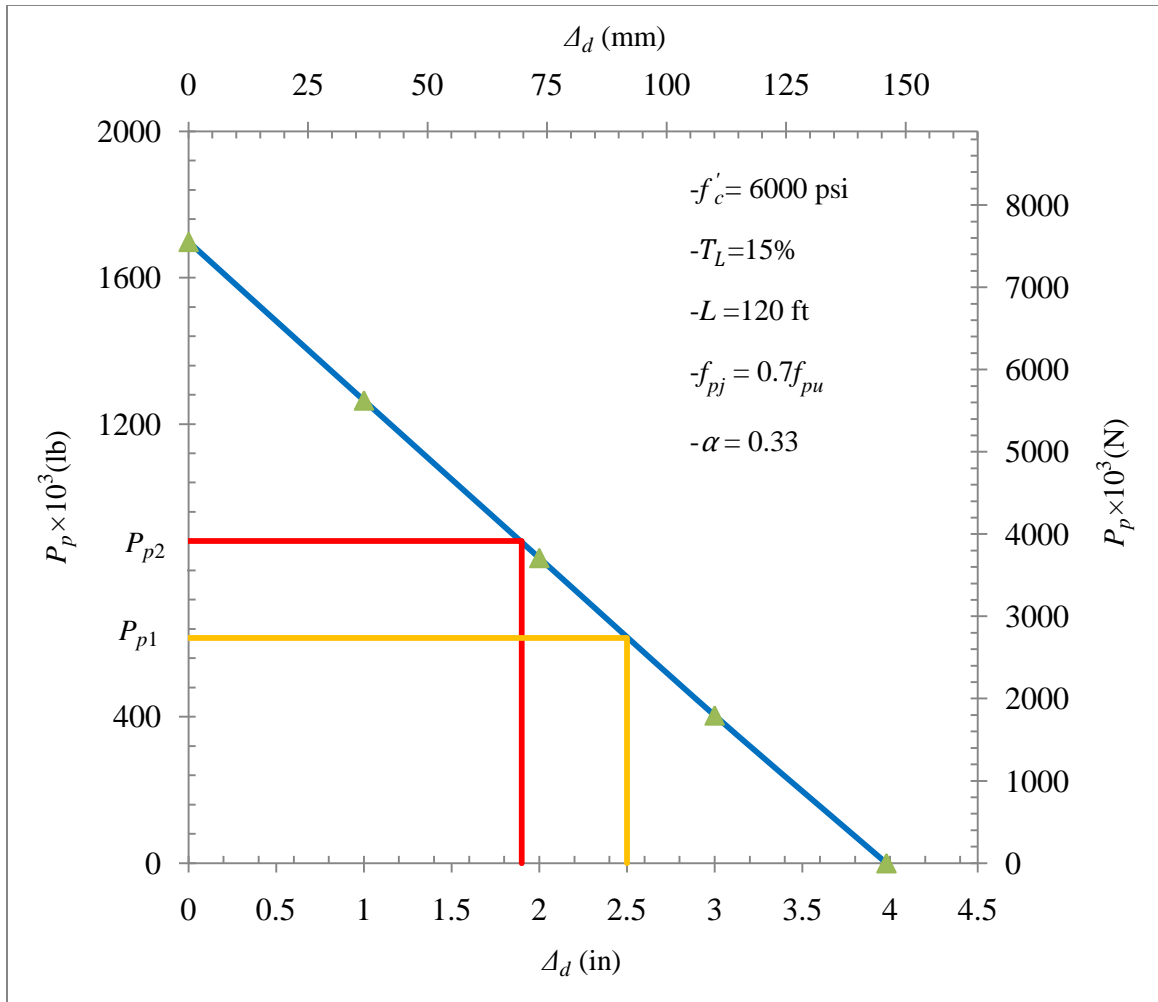


Figure 5.13 Variation of post tensioning Jacking force, P_p , with design camber, Δ_d , for pretensioning losses, $T_L=15\%$, for the PCI-8 girder

$$P_p = 2443 - 1097\alpha - 26.5T_L - \Delta_d(243.67 + 0.0303f'_c) \quad \text{Eq.5.12a}$$

Following the same procedure but using Eq.5.12a instead of Fig.1 will lead to,

$$P_{p1} = 2443 - 1097(0.33) - 26.5(15) - (2.5)[243.67 + 0.0303(6000)] = 619 \times 10^3 \text{ lb}$$

$$P_{p2} = 2443 - 1097(0.33) - 26.5(15) - (1.9)[243.67 + 0.0303(6000)] = 875 \times 10^3 \text{ lb}$$

$$P_p = 875 - 619 = 256 \times 10^3 \text{ lb}$$

5.6 Moment Capacity Reduction

In order to understand the effect of the post tensioning jacking force on the capacity of the cross section, moment- curvature diagrams have been generated after applying different levels of post tensioning jacking force. Also, relationships between the moment and net tensile strain are derived at different levels of post tensioning force to present the effect of the post tensioning jacking force on the strain level Fig.5.14 to 5.17.

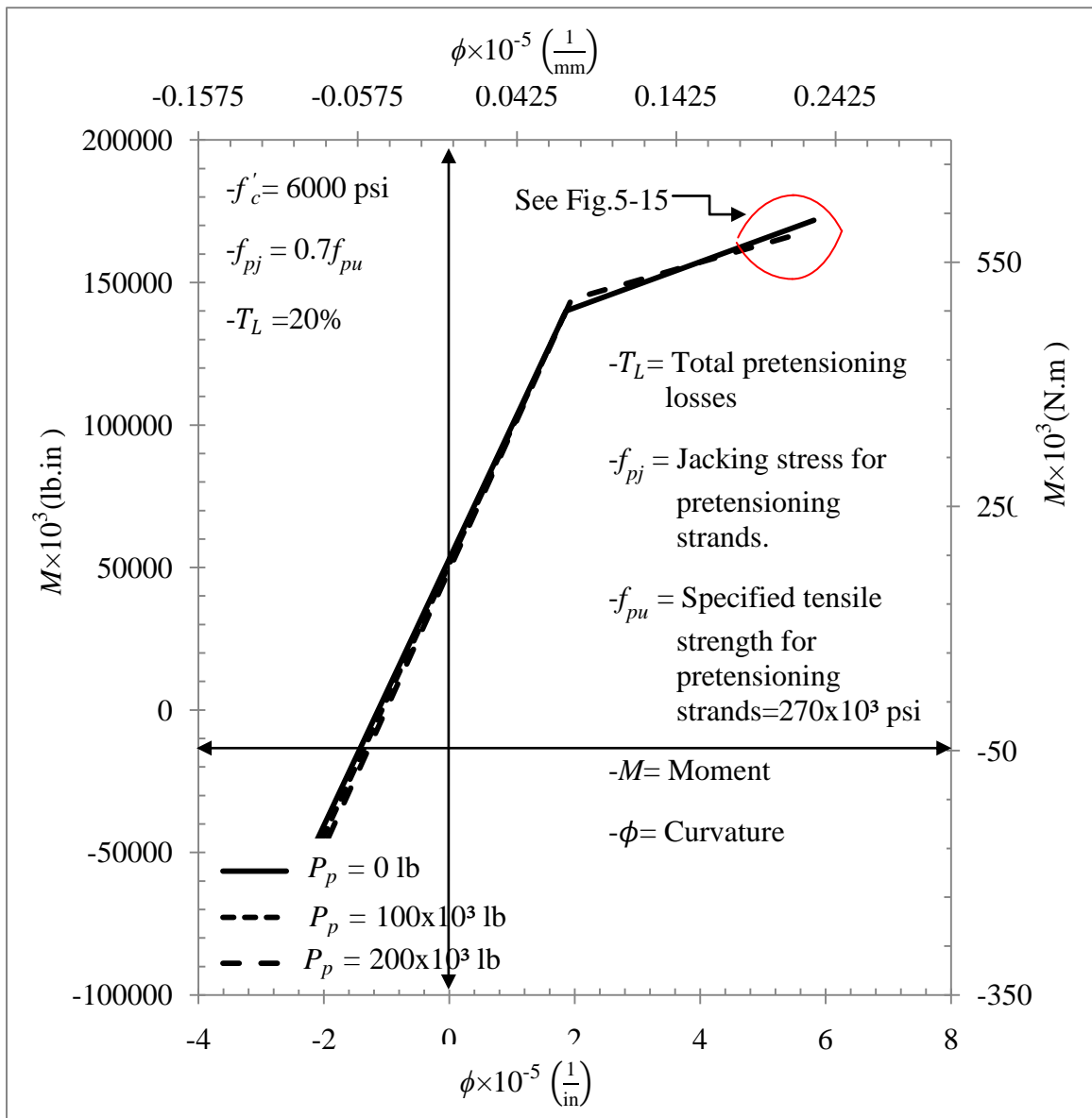


Figure 5.14 Moment- curvature, M - ϕ , interaction diagram for different post tensioning jacking force, P_p , for the PCI 8 girder

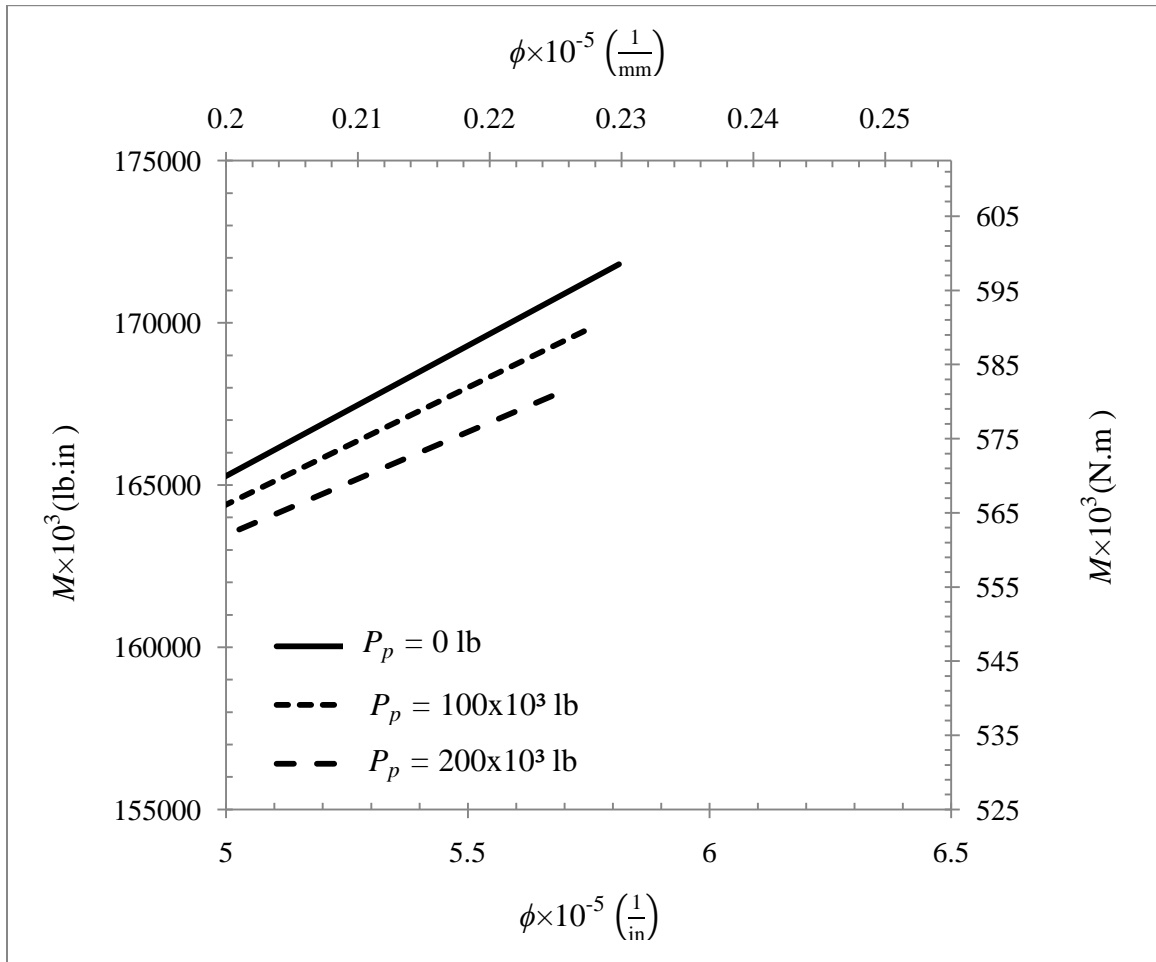


Figure 5.15 Moment- curvature, M - ϕ , interaction diagram for different post tensioning jacking force, P_p , for the PCI 8 girder

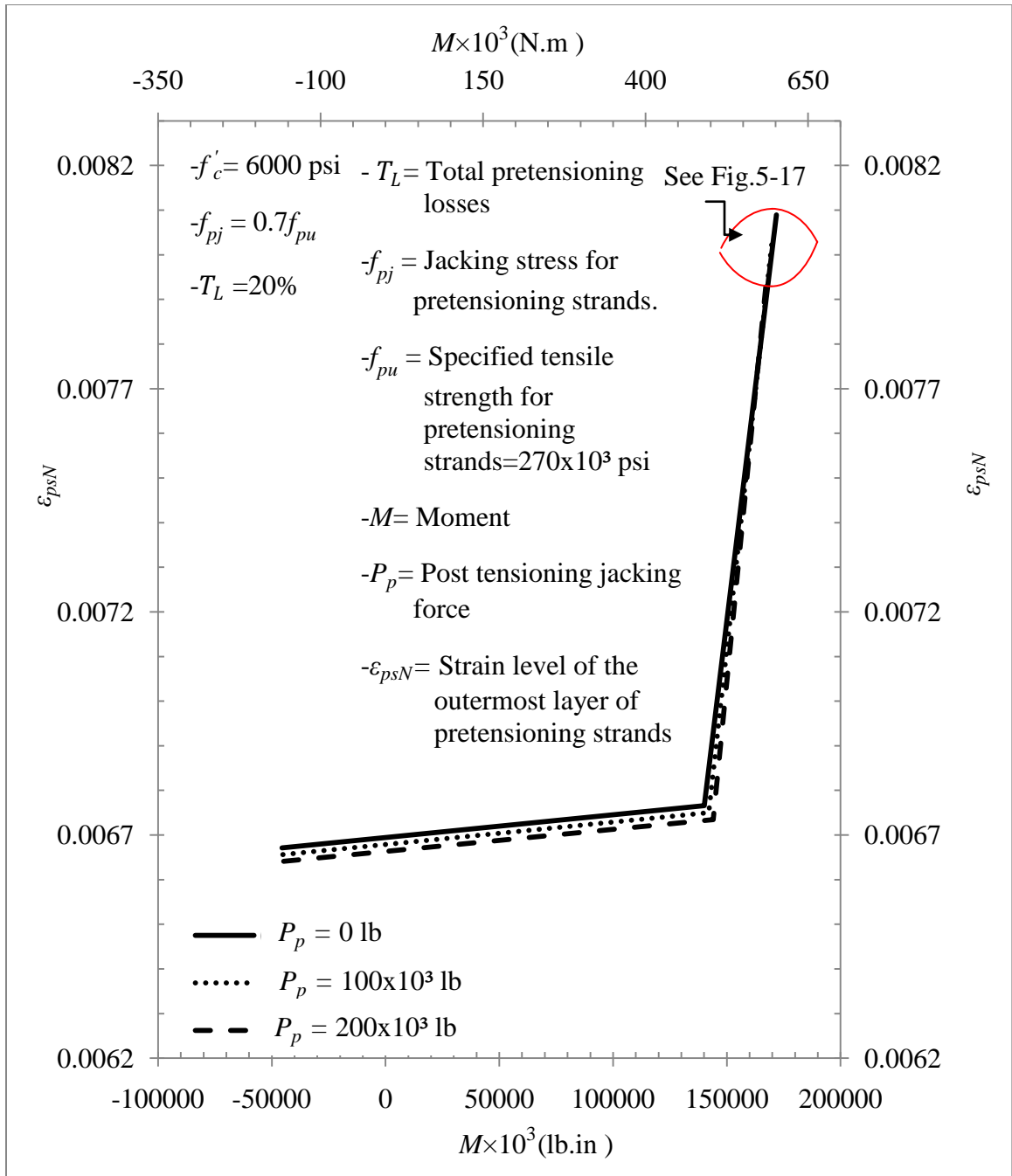


Figure 5.16 Moment vs. the strain of the outermost layer of pretensioning, $M-\epsilon_{psN}$, relationship for different post tensioning jacking force, P_p , for the PCI 8 girder

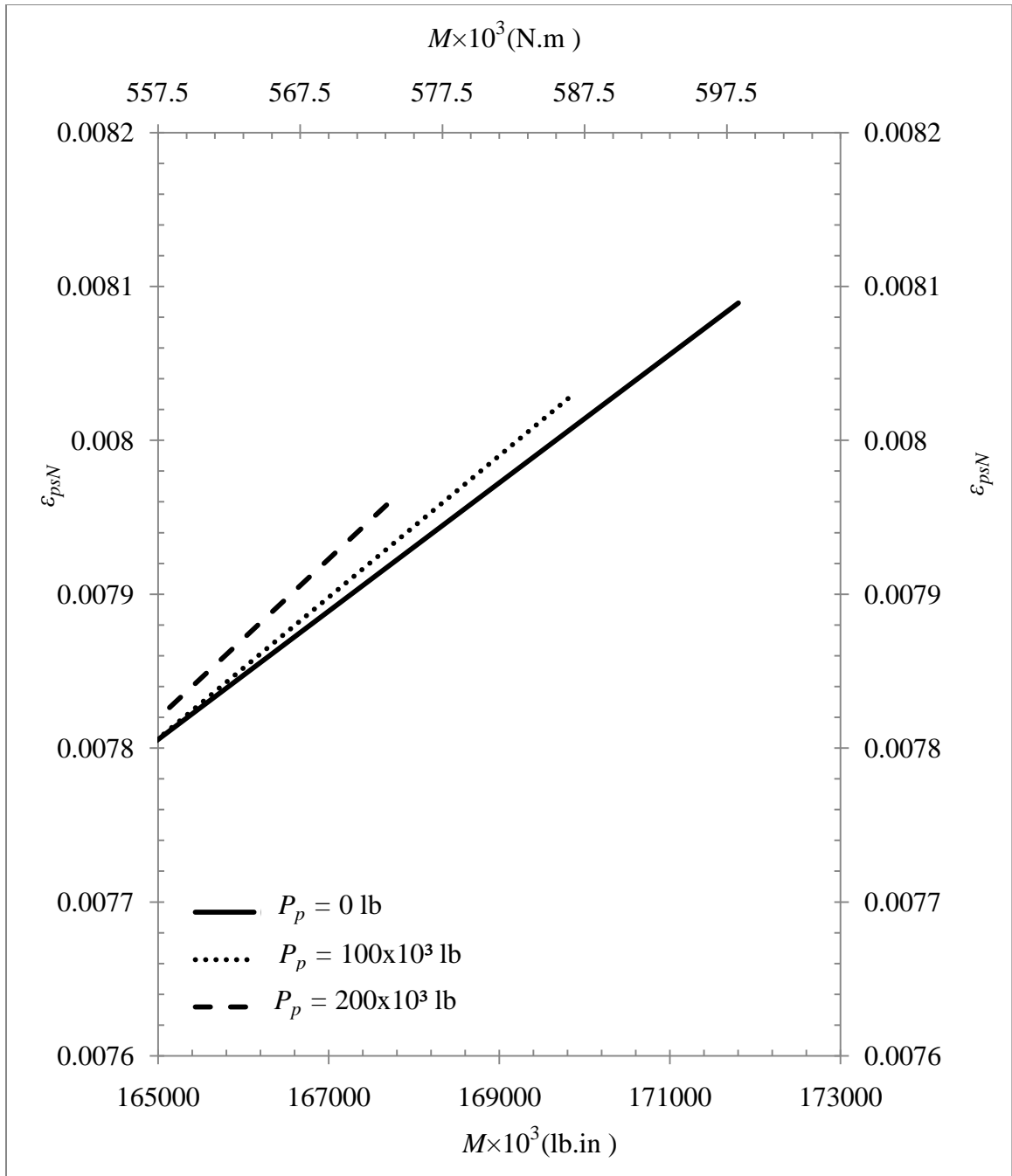


Figure 5.17 Moment vs. the strain of the outermost layer of pretensioning, M - ϵ_{psN} , relationship for different post tensioning jacking force, P_p , for the PCI 8 girder

5.7 Summary

This chapter presented the concept of using post tensioning strands to reduce camber in prestressed concrete bridge girders. Based on equilibrium conditions, strain compatibility, and material constitutive laws, the study generated relationships for the post tensioning jacking force vs. the design camber. Those relations are important to understand the behavior of the bridge girders. This study considered the effect of four variables: prestress losses, bridge girder length, specified concrete compression strength, and the distance coefficient of the c.g.s of the pretensioning strands. Also, this chapter presents findings regardless of the effect of the post tensioning jacking force on the moment capacity of the bridge girders. These findings are listed below:

- 1- The post tensioning jacking force required producing a specific design camber varies linearly with the design camber
- 2- The PCI-8, ASSHTO type-4, and ASSHTO B54x48 box beam tends t have higher camber with higher specified concrete compression strength
- 3- Using a higher distance coefficient α required higher post tensioning jacking force to produce the same design camber
- 4- Results obtained from equations derived to represent relationships between the post tensioning jacking force and the design camber coincide with the actual data obtained from the study
- 5- The reduction in the moment capacity per 100×10^3 lb of applied post tensioning jacking force is 1.15% for the PCI-8 girder, 2.9% for the AAHTO type-4 girder, and 0.33% for the AASTO b54x48 box beam

CHAPTER 6

CONCLUSION AND RECOMMENDATIONS

6.1 Conclusion and Findings

The post tensioning strands is a viable method to reduce camber in PCI-8, ASSHTO type-4, and ASSHTO B54x48 box beam. The major findings based on the results of the research reported in this thesis are presented as follows:

- 1- The post tensioning jacking force required producing a specific design camber varies linearly with the design camber
- 2- Using higher compressive strength of concrete reduces the amount of post tensioning force
- 3- Using a higher distance coefficient α increases the post tensioning jacking force
- 4- The highest reduction in the moment capacity is taken place for the AASHTO type-4 girder by 2.9% per 100×10^3 of post tensioning jacking force

6.2 Future Work

- 1- For future work, other types of bridge girders could be considered
- 2- The Hognestad stress-strain model for short term monotonic was adopted in this study. However, other models should be used to account for shrinkage and creep in concrete
- 3- A detailed cost analysis should be done since placement of post tensioning strands increases the material and labor costs of the bridge girder
- 4- Camber control cracked concrete bridge girders could be considered as a future work

APPENDIX A

Appendix A contains the figures representing the relationships between the post tensioning jacking force and the design camber depending on the total losses, span length, concrete strength, and distance coefficient, α . In addition, it contains data sheets showing the dimension details and number of strands used in the PCI 8 girder, AASHTO type-4 girder, and AASHTO B54x48 box beam.

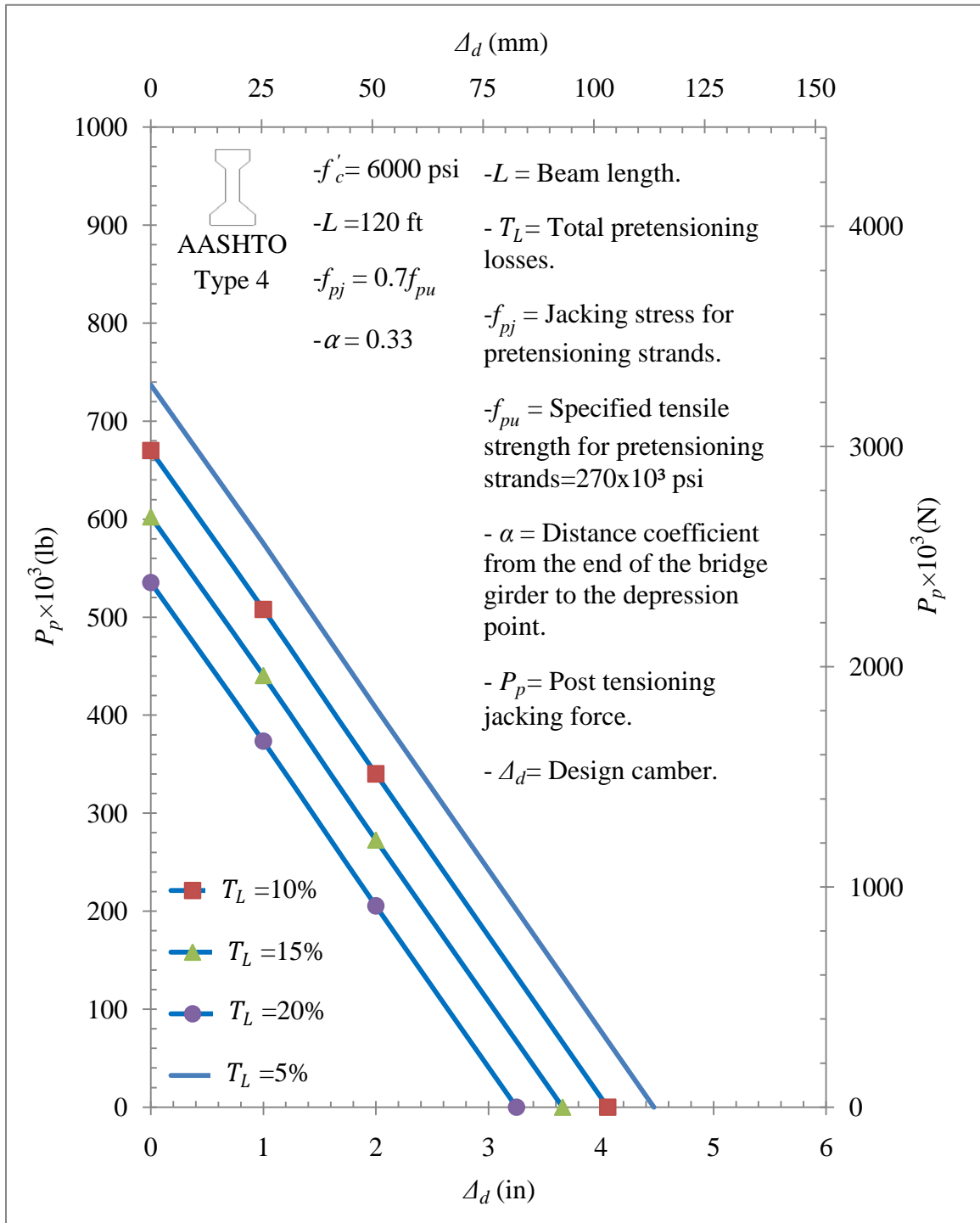


Figure A.1 Post tensioning Jacking force, P_p , vs. design camber, Δ_d , for different prestressing losses, T_L , for the AASHTO type-4 girder

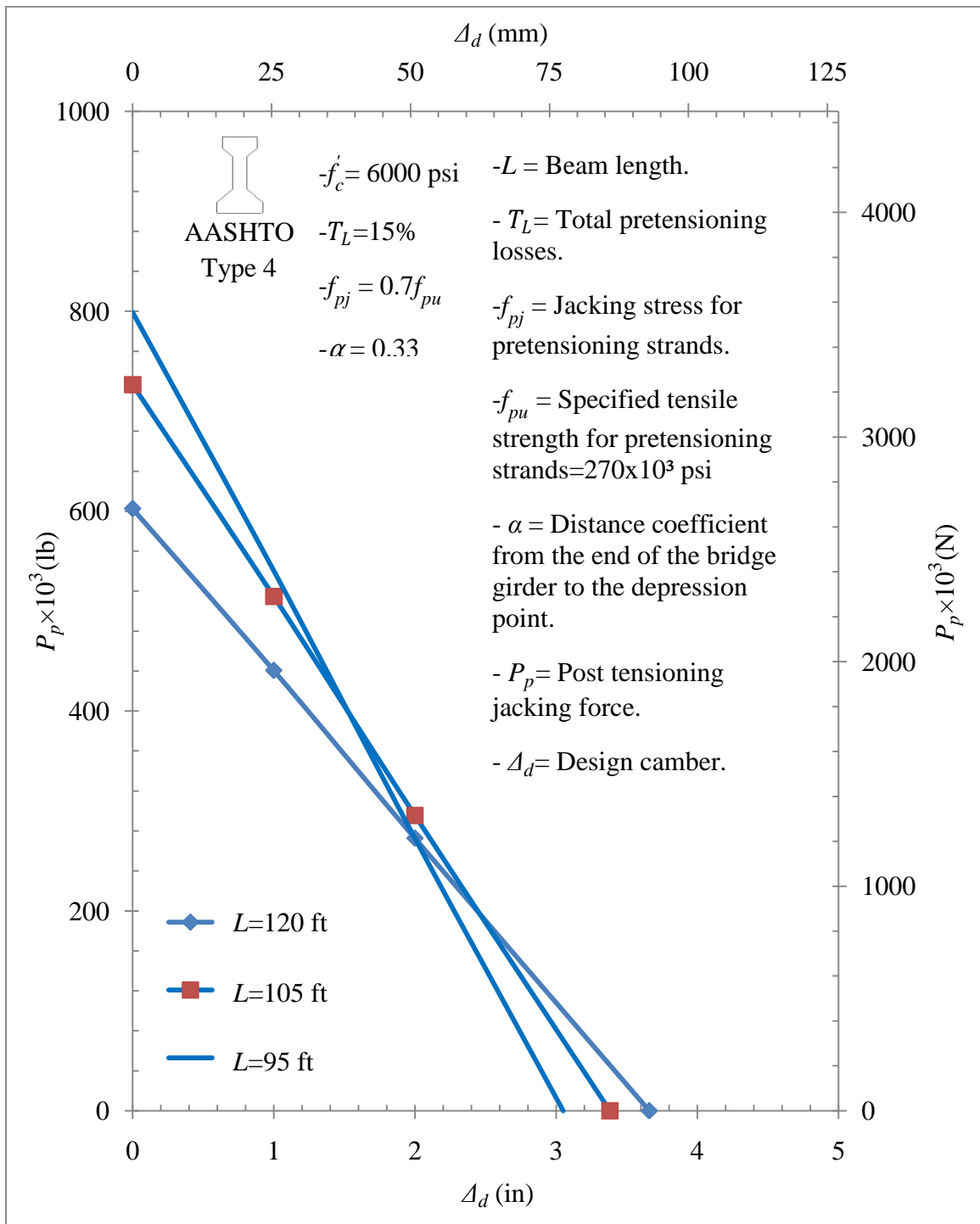


Figure A.2 Variation of post tensioning Jacking force, P_p , with design camber, Δ_d , for different bridge girder length, L , for the AASHTO type-4 girder

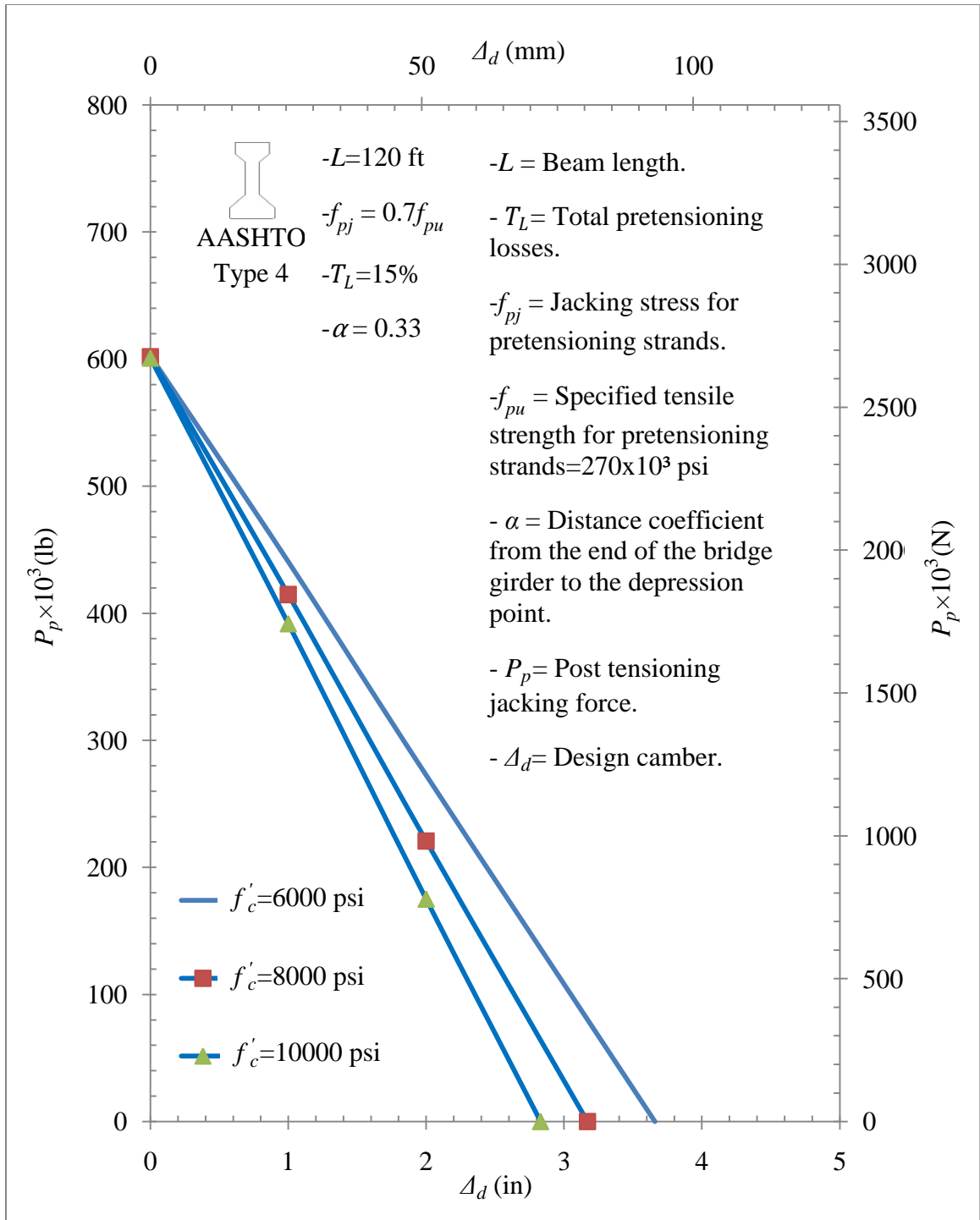


Figure A.3 Variation of post tensioning Jacking force, P_p , with design camber, Δ_d , for different beam length, f'_c , for the AASHTO type-4 girder

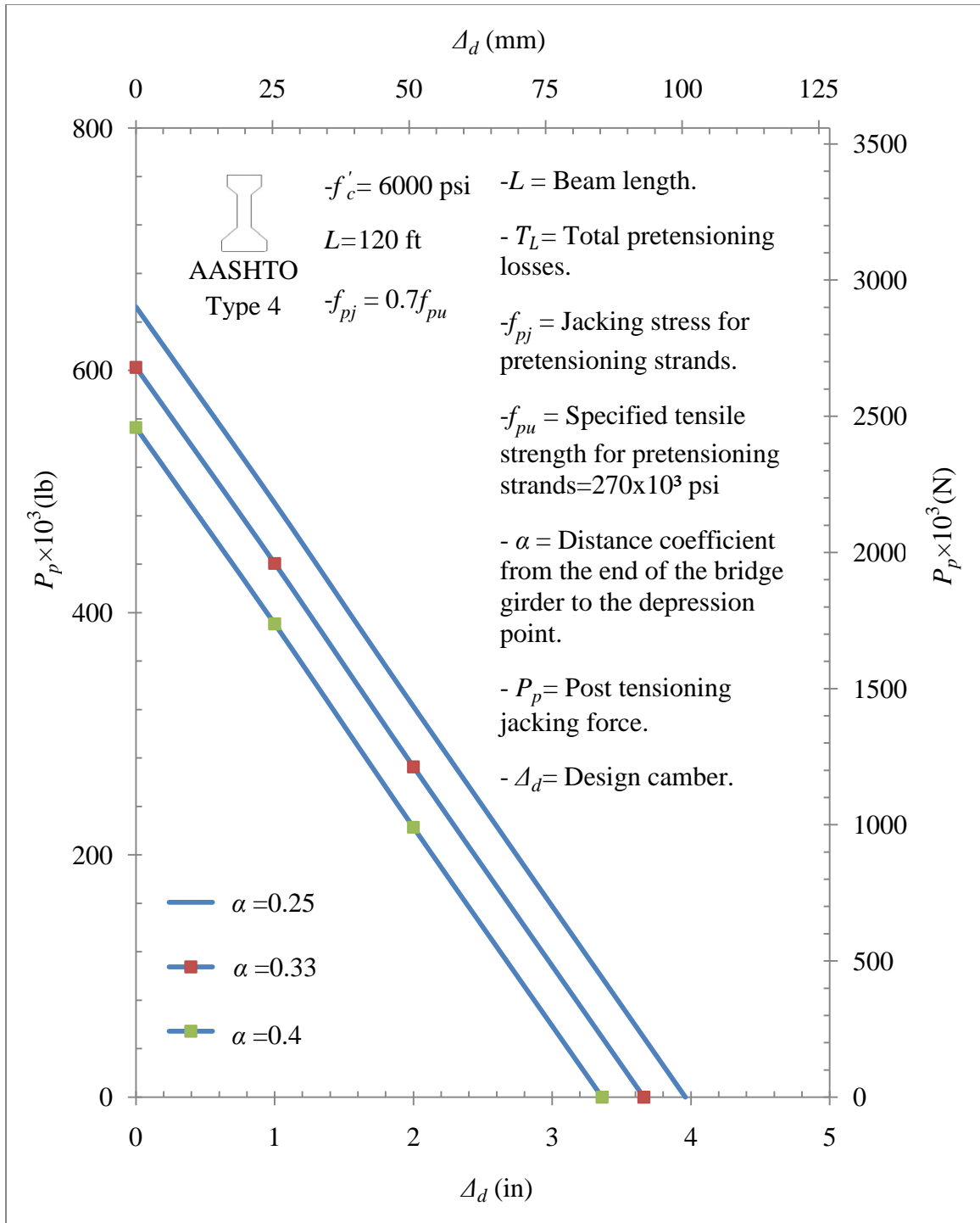


Figure A.4 Post tensioning Jacking force, P_p , vs. design camber, Δ_d , for different distance coefficient, α , for the AASHTO type-4 girder

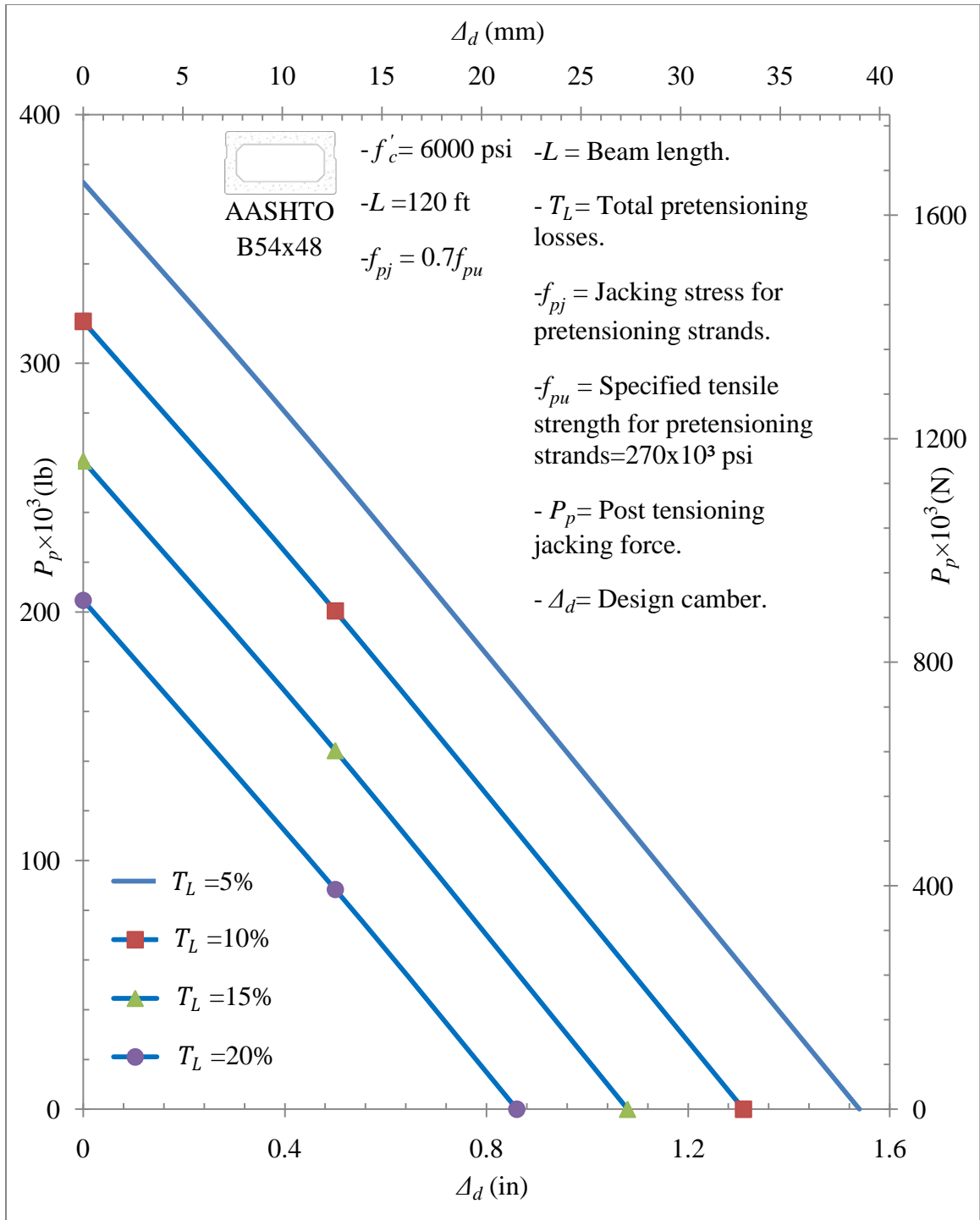


Figure A.5 Post tensioning Jacking force, P_p , vs. design camber, Δ_d , for different pretensioning losses, T_L , for the AASHTO B54x48 box beam

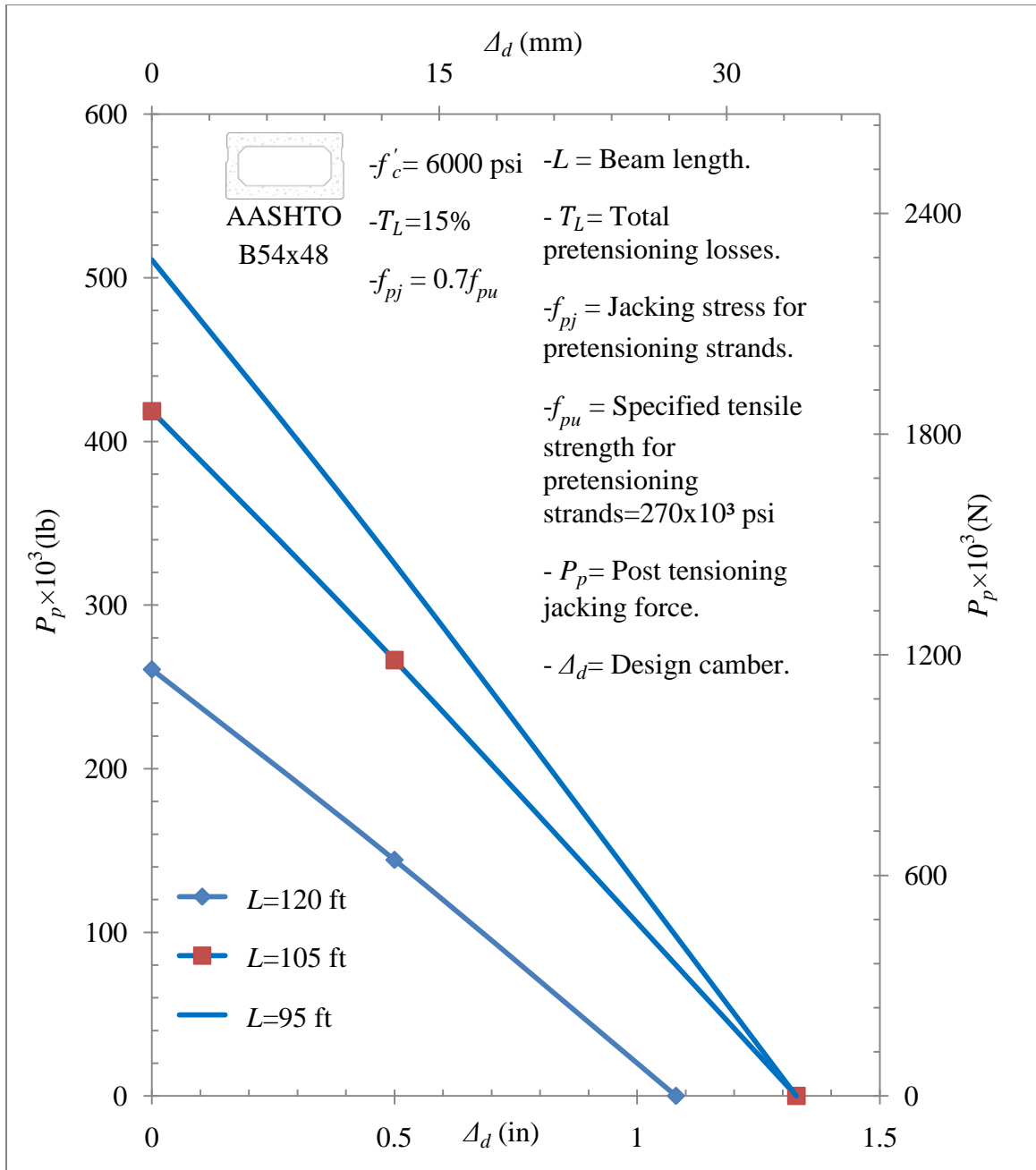


Figure A.6 Variation of post tensioning Jacking force, P_p , with design camber, Δ_d , for different bridge girder length, L , for the AASHTO B54x48 box beam

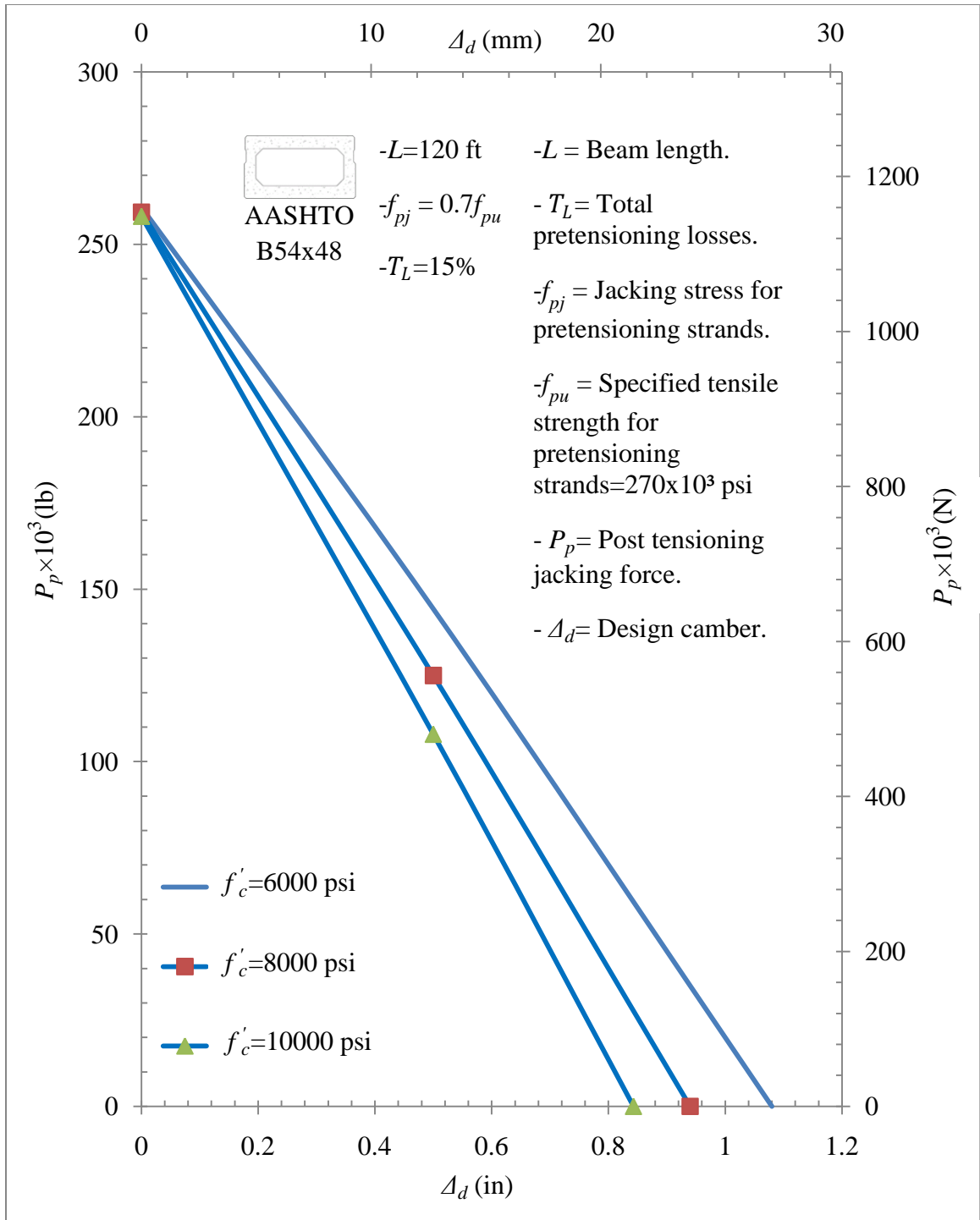


Figure A.7 Variation of post tensioning Jacking force, P_p , with design camber, Δ_d , for different specified concrete strength, f'_c , for the AASHTO B54x48 box beam

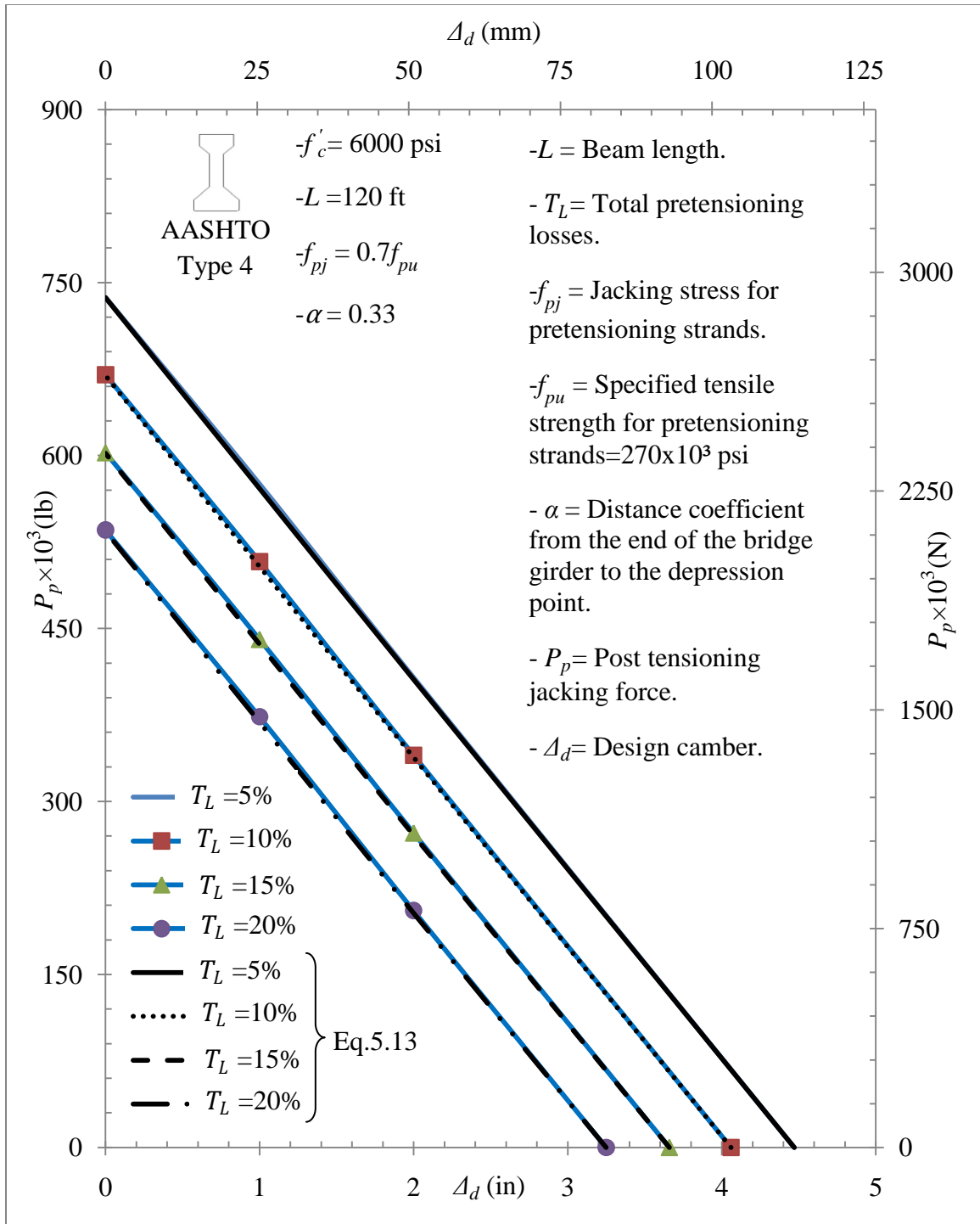


Figure A.8 Comparison between results obtained from the study and Eq.5-13 for different pretensioning losses, T_L , for the AASHTO type-4 girder

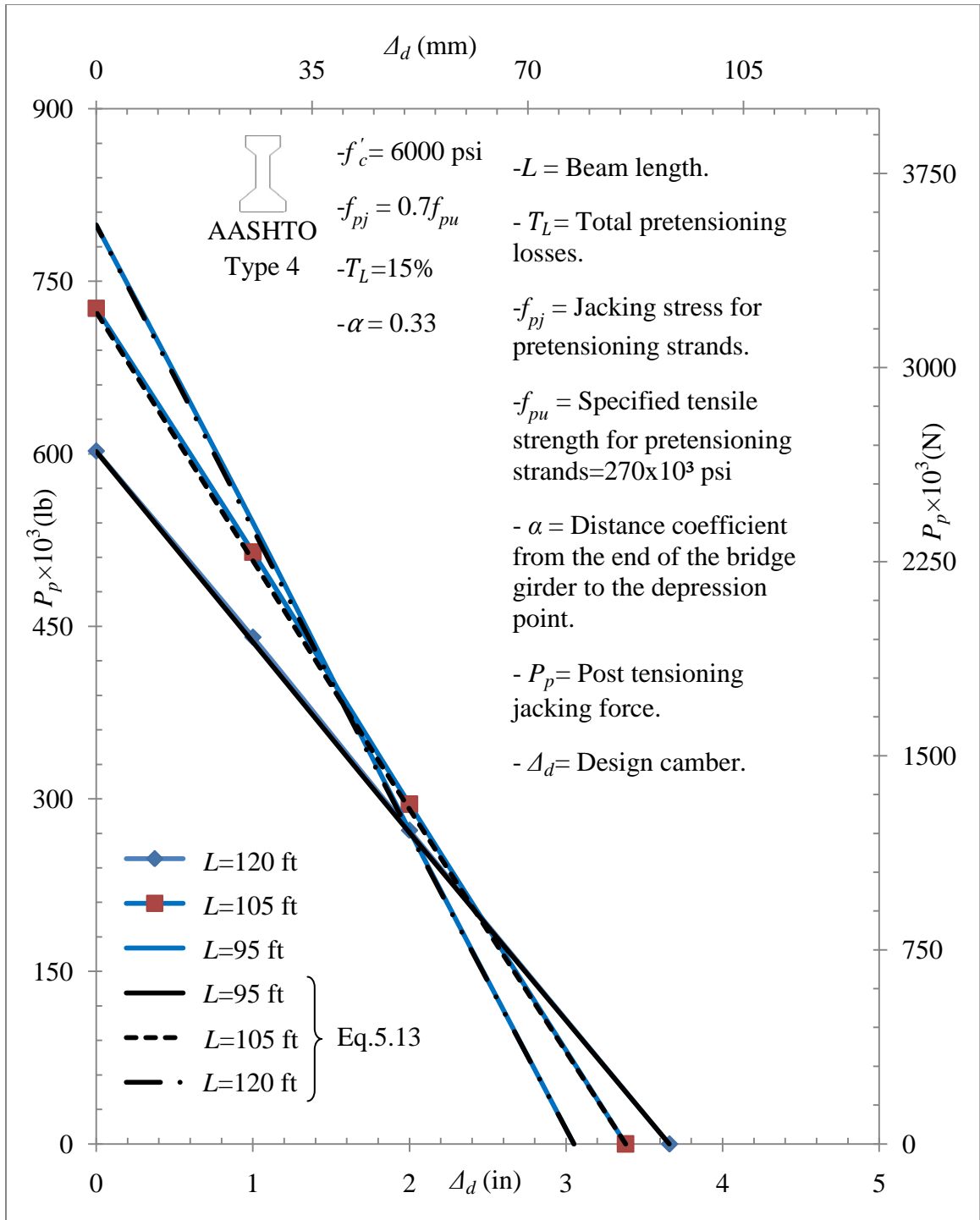


Figure A.9 Comparison between results obtained from the study and Eq.5-13 for different bridge girder length, L , for the AASHTO type-4 girder

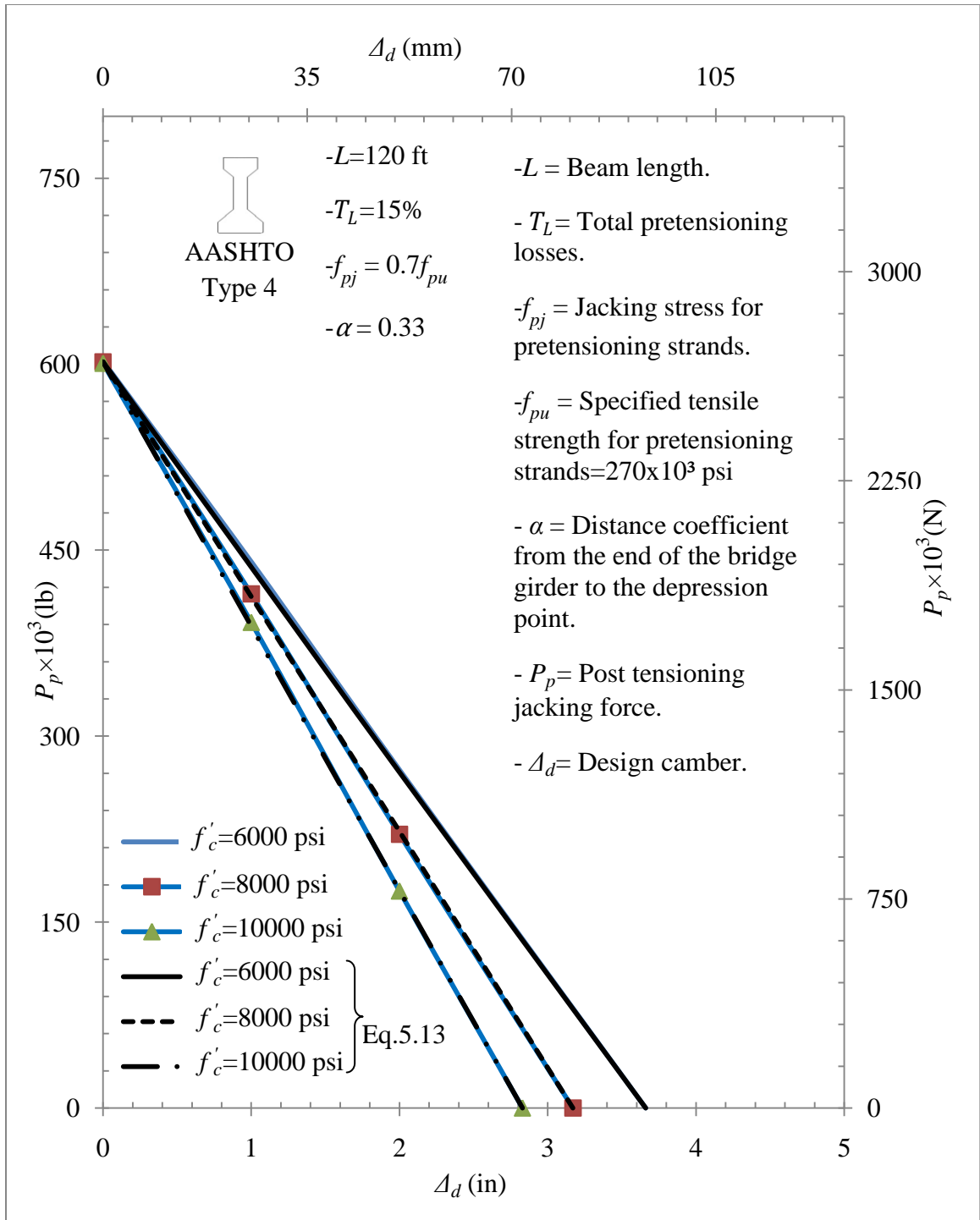


Figure A.10 Comparison between results obtained from the study and Eq.5-13 for different specified concrete strength, f'_c , for the AASHTO type-4 girder

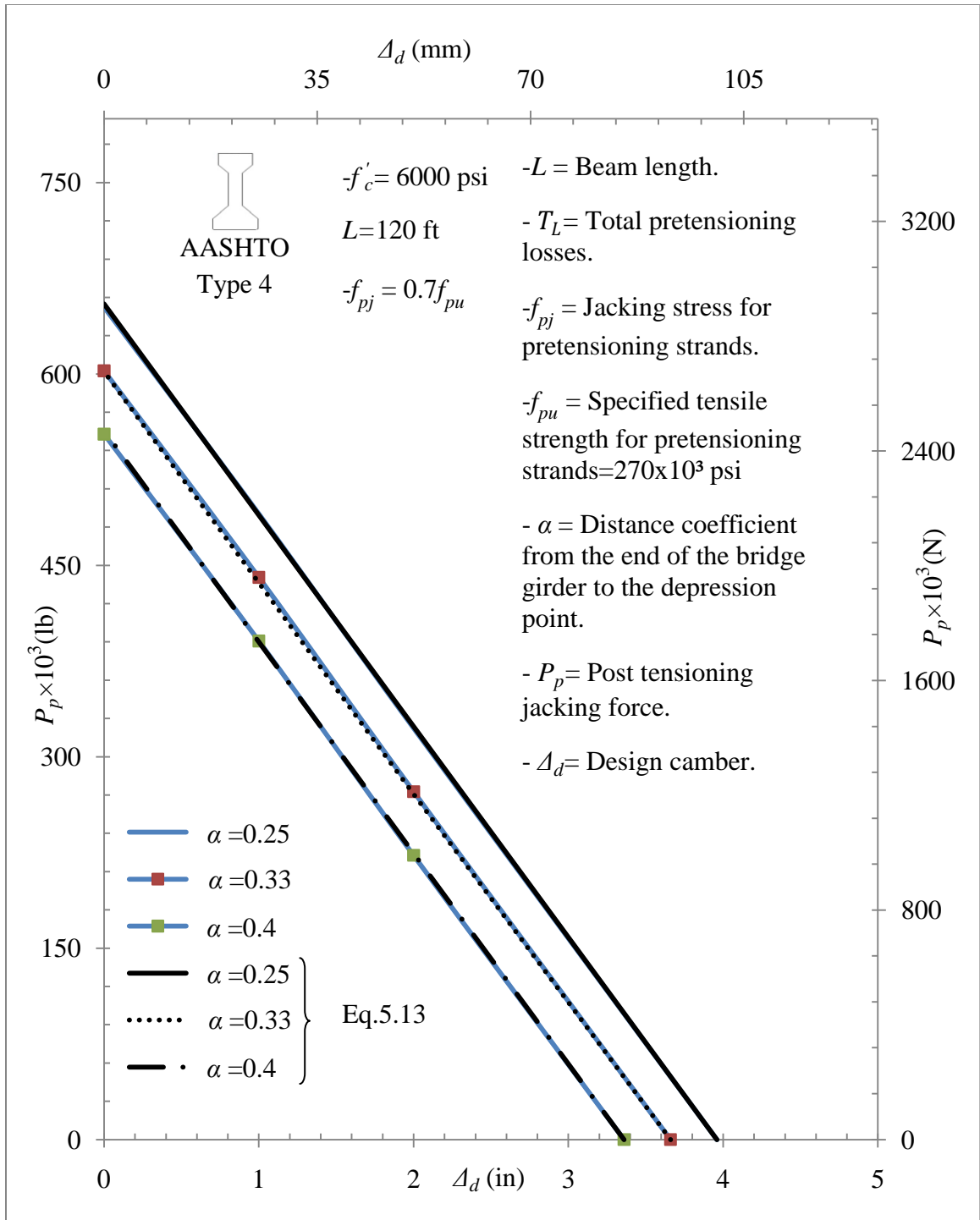


Figure A.11 Comparison between results obtained from the study and Eq.5-13 for different distance coefficient, α , for AASHTO type-4 girder

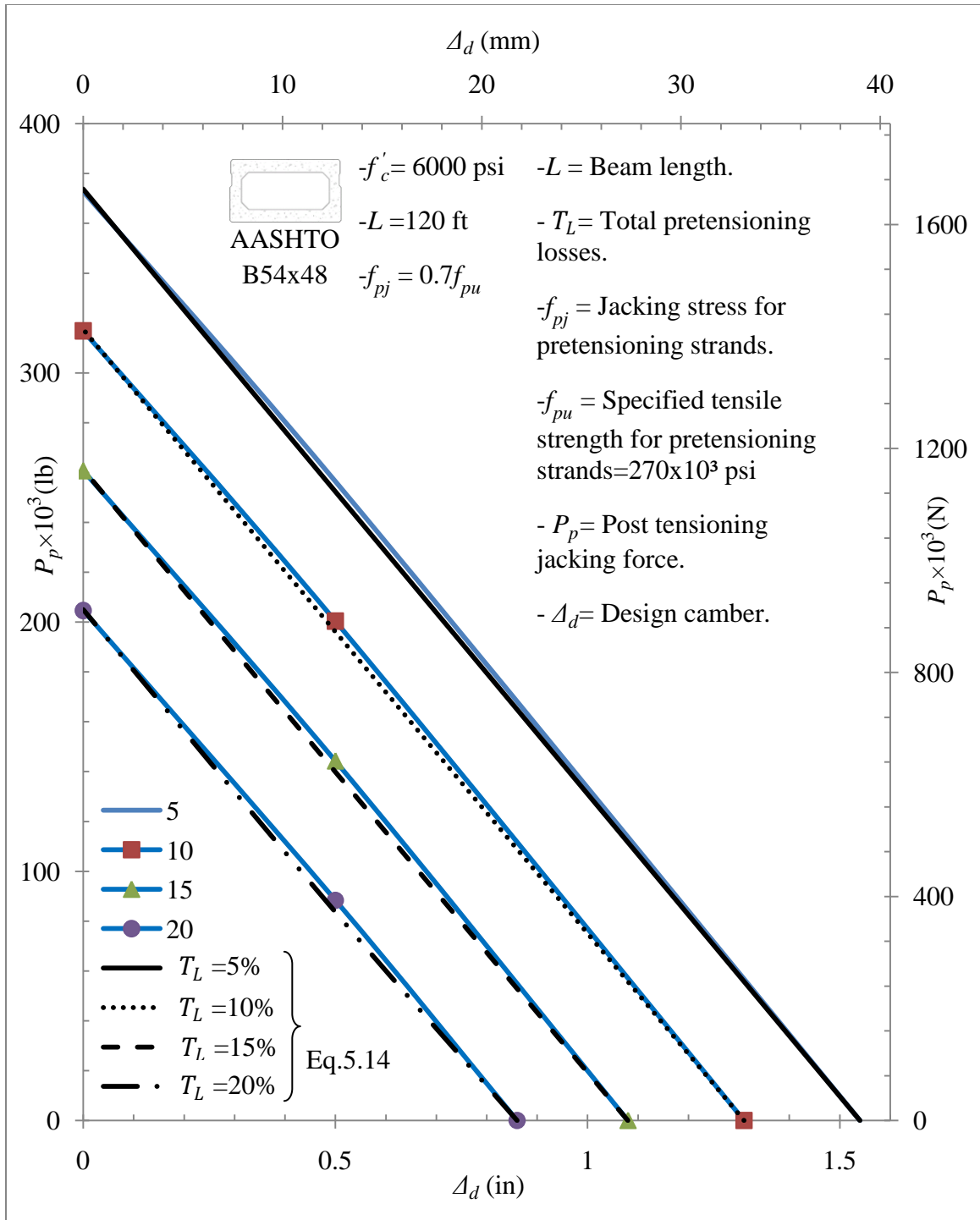


Figure A.12 Comparison between results obtained from the study and Eq.5-14 for different pretensioning losses, T_L , for the AASHTO B54x48 box beam

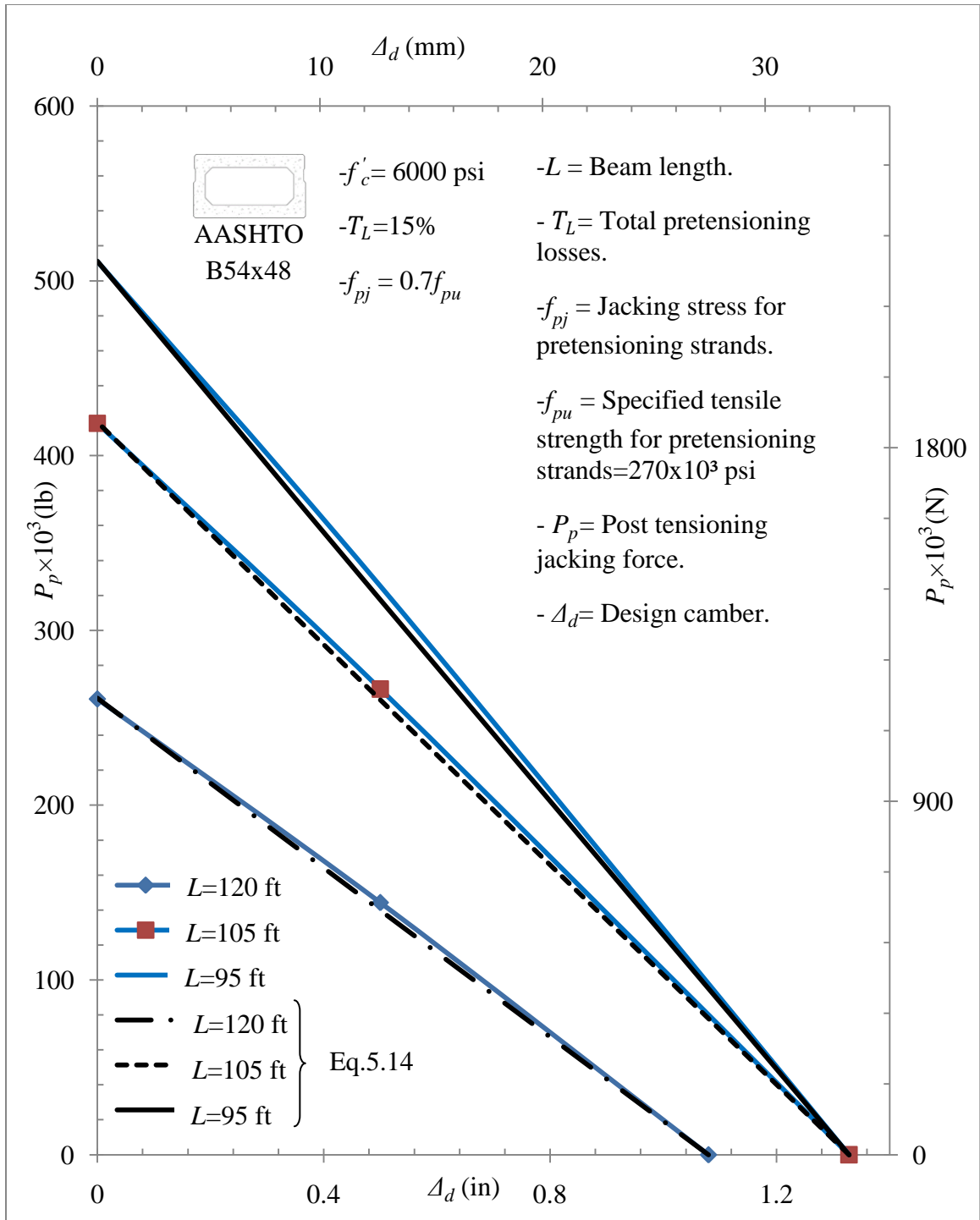


Figure A.13 Comparison between results obtained from the study and Eq.5-14 for different bridge girder length, L , for the AASHTO B54x48 box beam

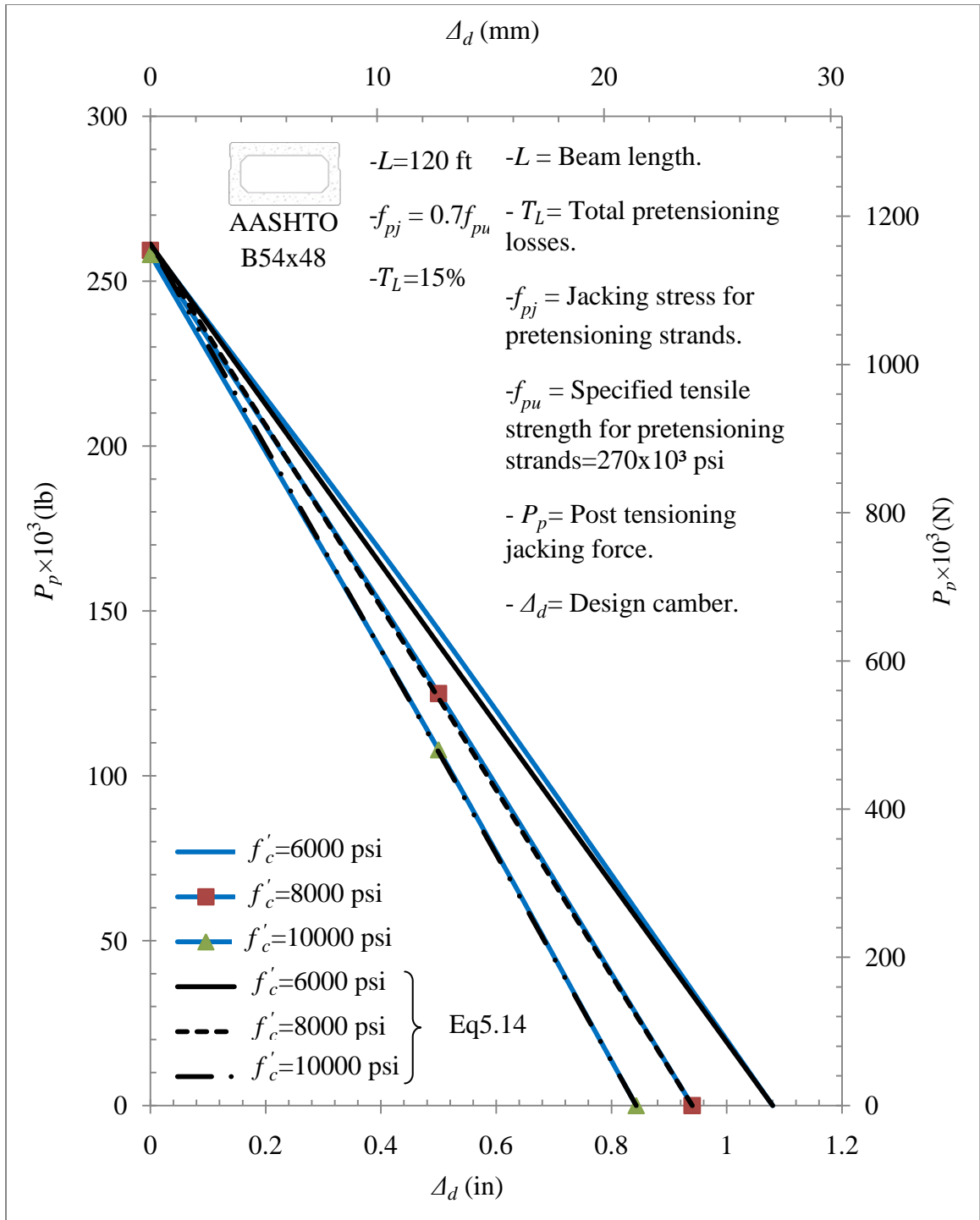


Figure A.14 Comparison between results obtained from the study and Eq.5-14 for different specified concrete strength, f'_c , for AASHTO B54x48 box beam

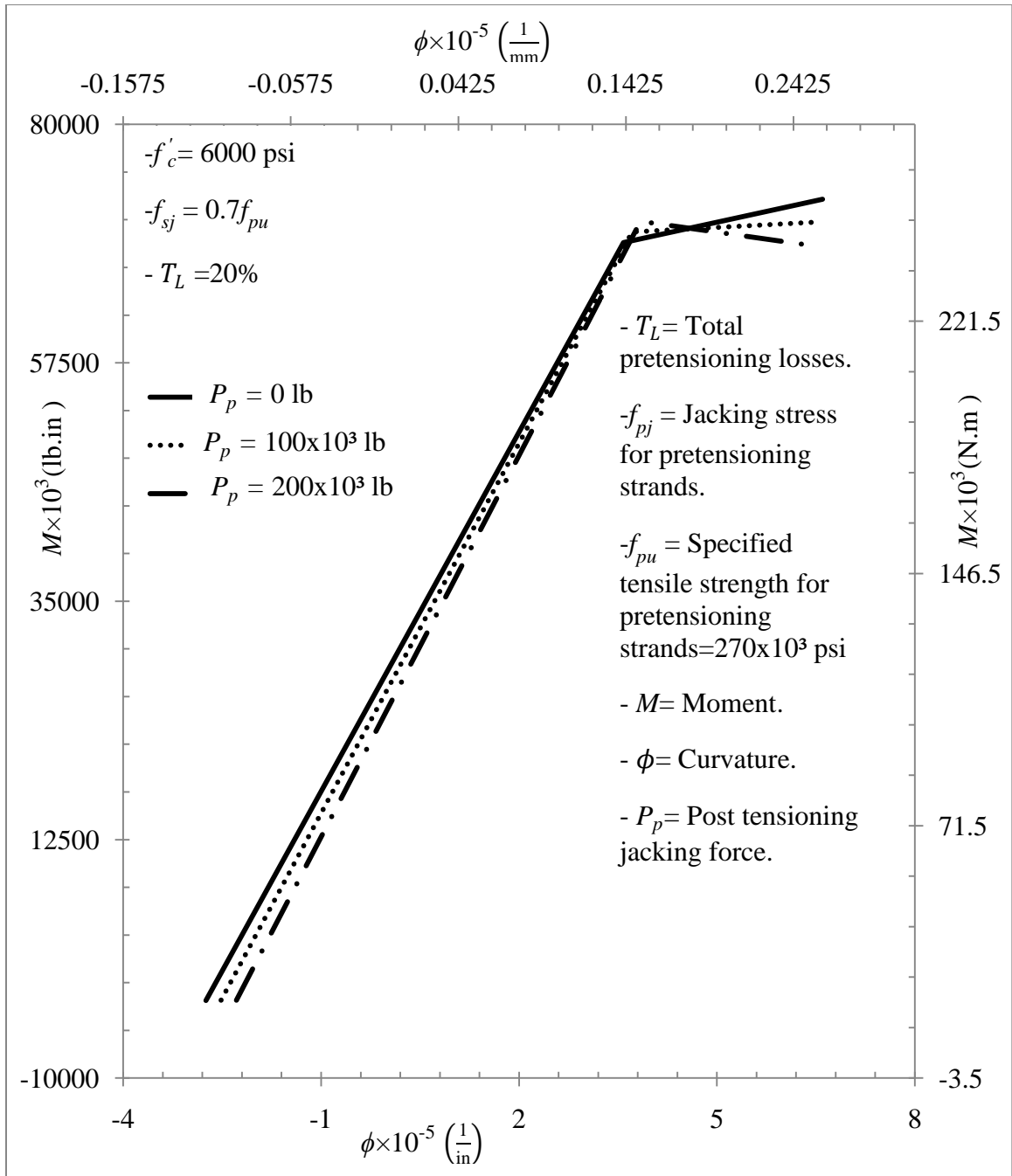


Figure A.15 Moment- curvature, M - ϕ , interaction diagram for different post tensioning jacking force, P_p , for the AASHTO type-4 girder

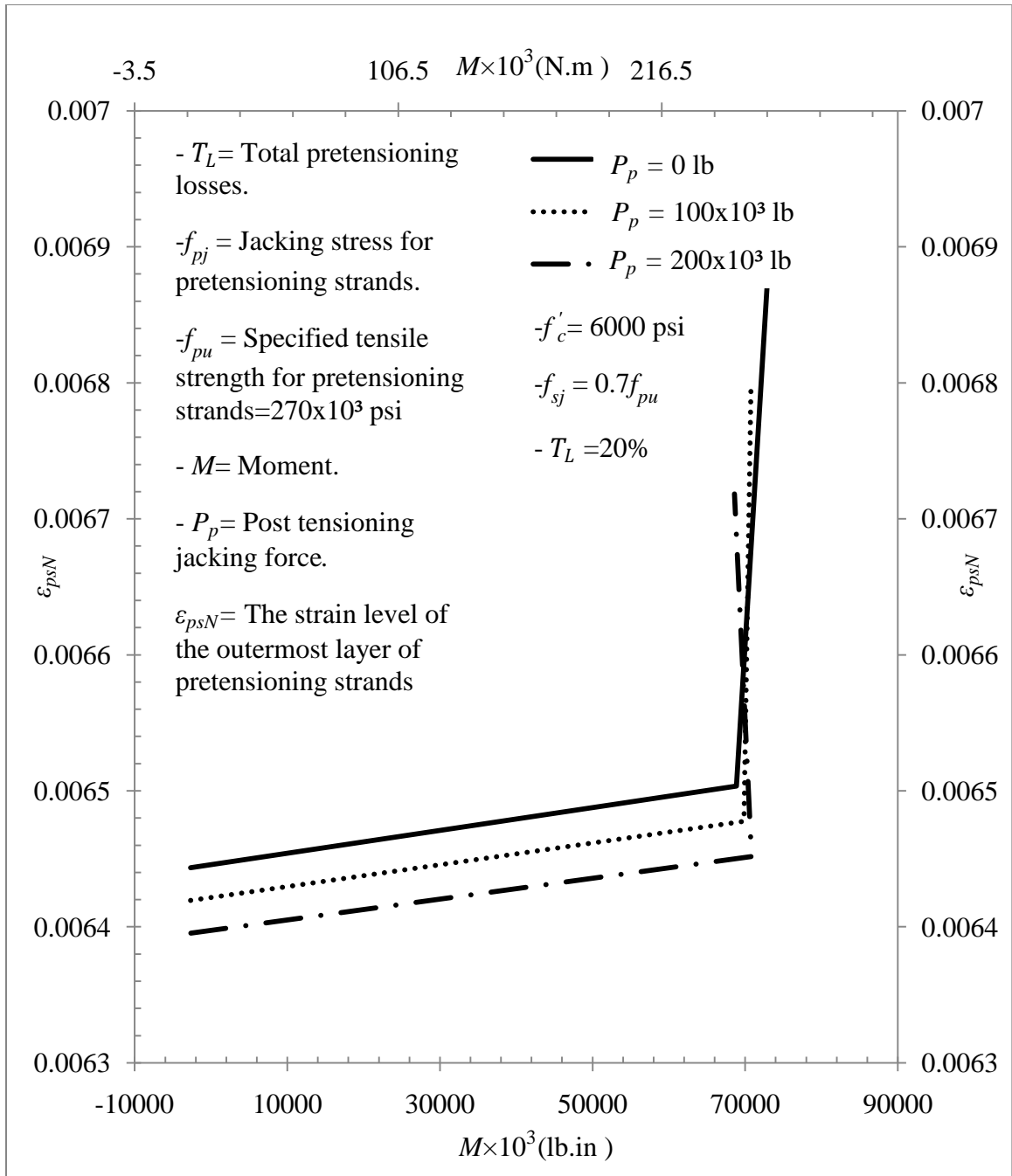


Figure A.16 Moment vs. the strain of the outermost layer of pretensioning, $M-\varepsilon_{psN}$, relationship for different post tensioning jacking force, P_p , for the AASHTO type-4 girder

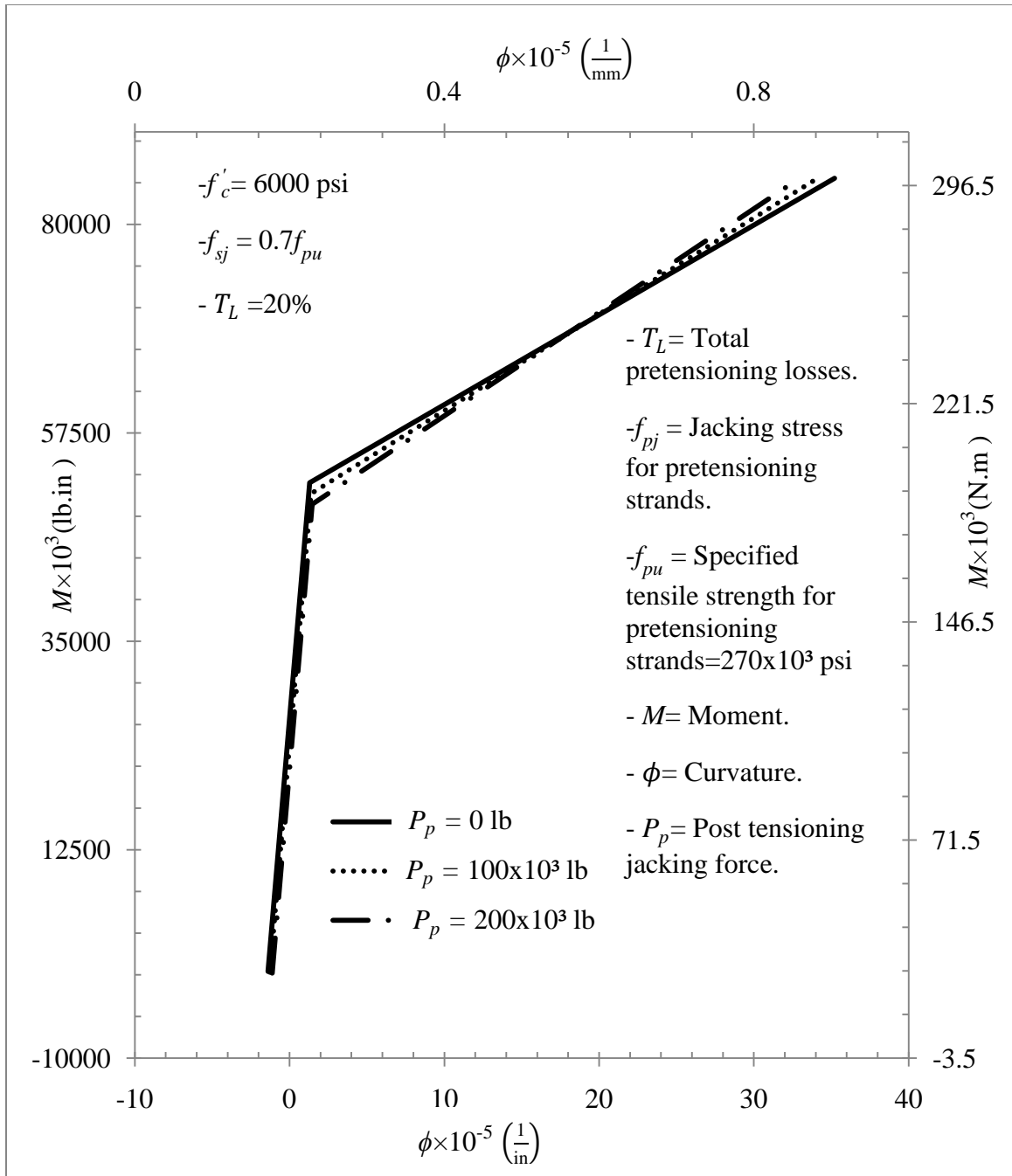


Figure A.17 Moment - curvature, M - ϕ , interaction diagram for different post tensioning jacking force, P_p , for the AASHTO B54x46 box beam

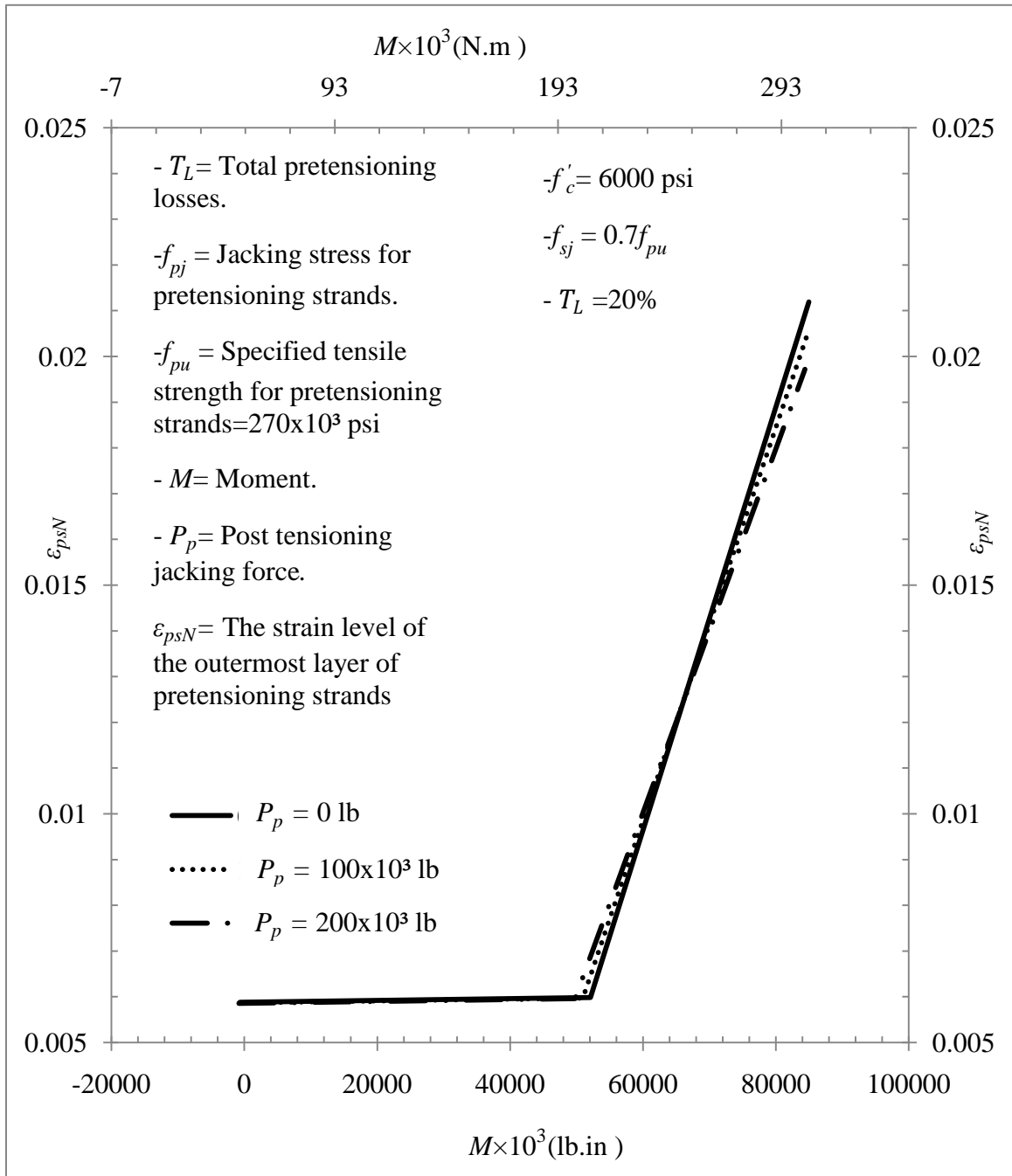
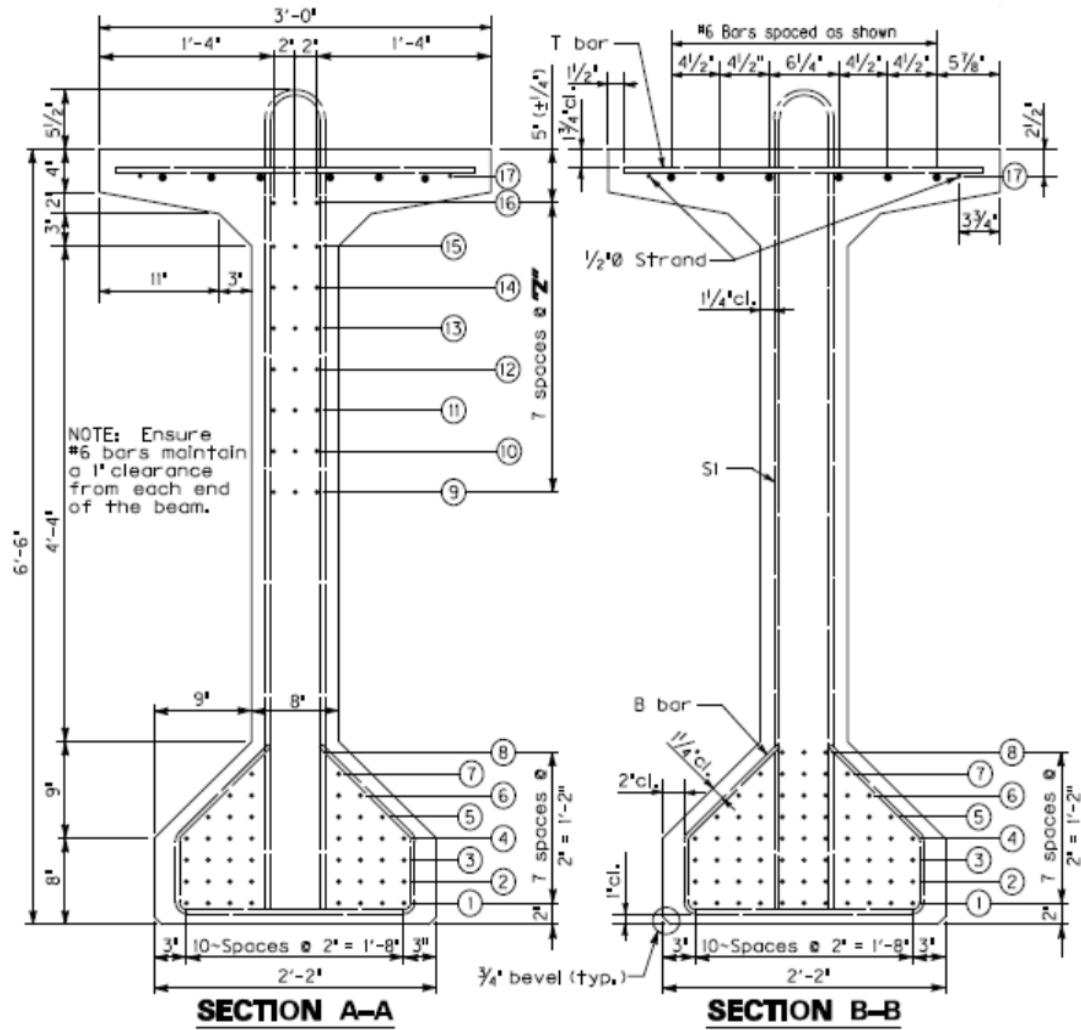


Figure A.18 Moment vs. the strain of the outermost layer of pretensioning, $M-\epsilon_{psN}$, relationship for different post tensioning jacking force, P_p , for AASHTO B54x48 box beam

STRAND SPLICE DETAIL



Strand Data with number indicated in rows	
Midspan (SECTION B-B)	End (SECTION A-A)

Figure A.19 Dimensions and reinforcement layout for PCI 8 girder (source: Division of Structural Design, Department of Highways, Commonwealth of Kentucky)

PRESTRESS SERVICES

INDUSTRIES LLC

Lexington, Ky - Decatur, In - Melbourne, Ky - Columbus, Oh - Henderson, Ky
859.299.0461 - 260.724.7117 - 859.441.0068 - 614.871.2900 - 270.826-6244

AASHTO Type 4 I-Beam Reinforcement Details

Product Code	Depth (in)	Area (in ²)	Y_b (in ⁴)	I_{xx} (in ⁴)	I_{yy} (in ⁴)	Weight (plf)
4I	54	788.4	24.8	260,403	24,282	822

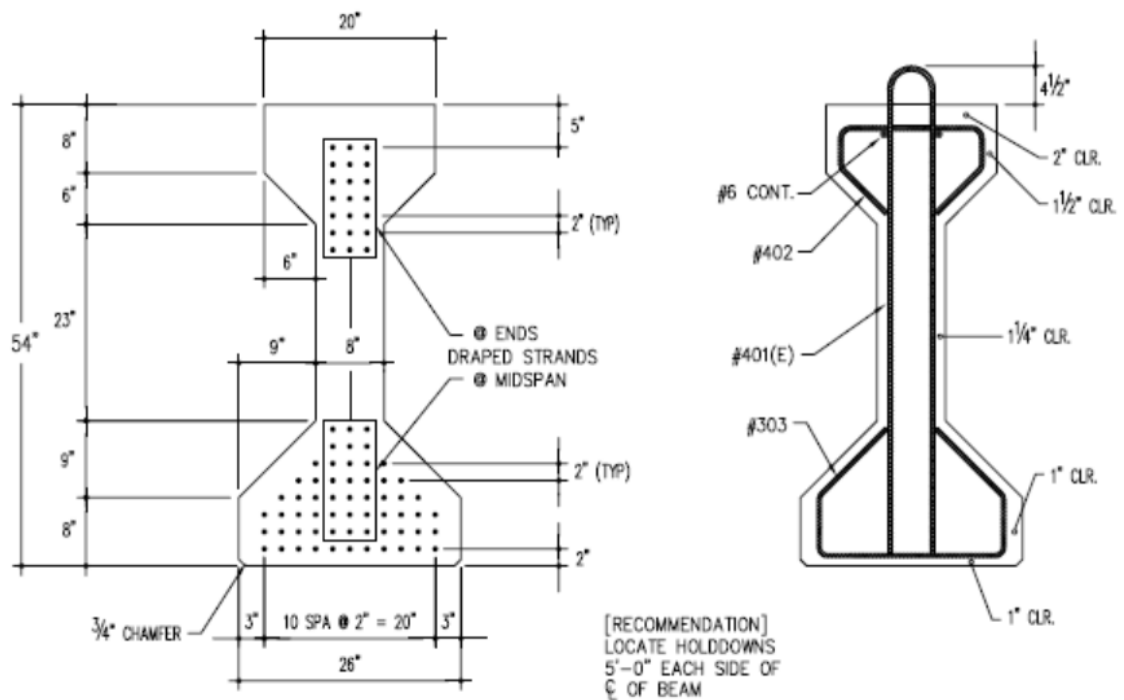


Figure A.20 Dimensions and reinforcement layout for AASHTO type-4 girder
(source: <http://www.prestressservices.com/products/bridge>)

B54 x 48 Box Beam Reinforcement Details

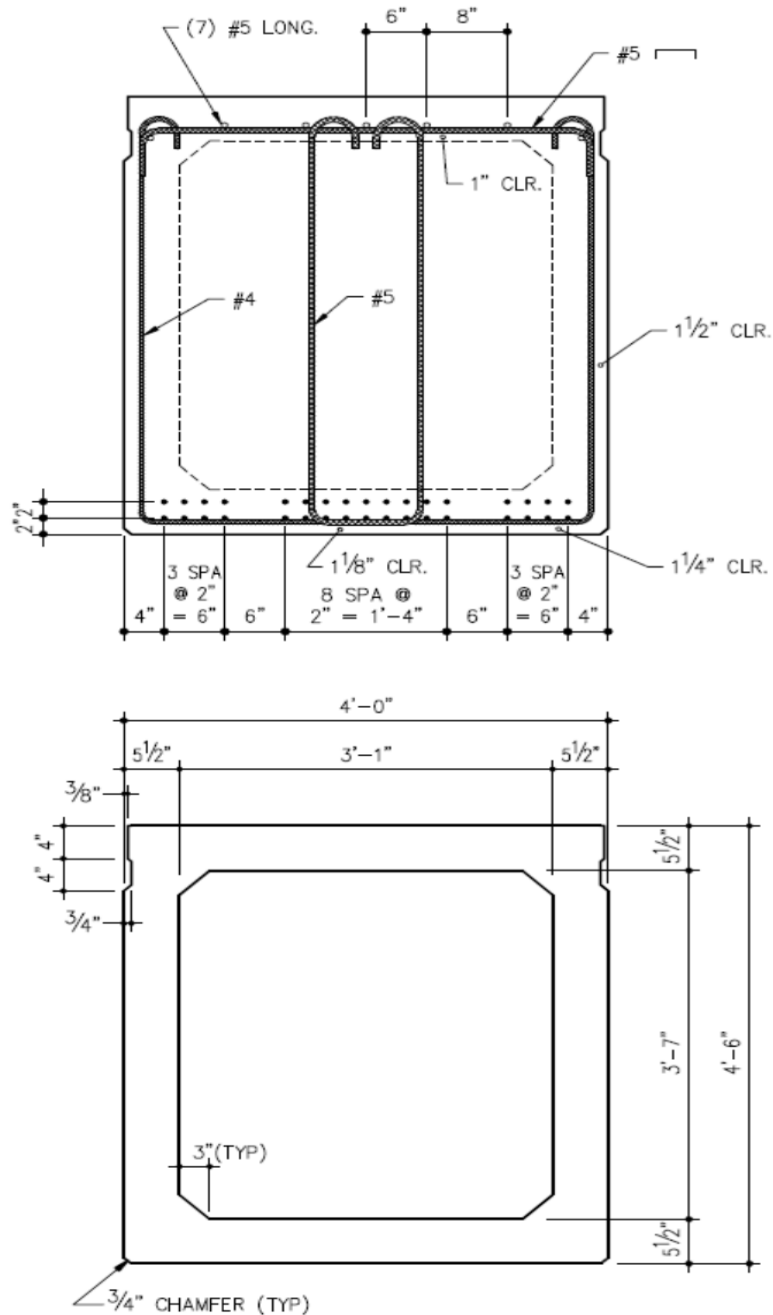


Figure A.21 Dimensions and reinforcement layout for AASHTO B54x48 box beam (source: <http://www.prestressservices.com/products/bridge>)

APPENDIX B

NOTATION

a	= distance from end of the beam to the depression
A_g	= area of concrete section
A_{ps}	= area of prestressing steel in flexure tension zone
A_s	= area of nonprestressed longitudinal tension reinforcement
A'_s	= area of compression reinforcement
b	= width of cross section
d	= distance from extreme compression fiber to centroid of longitudinal tension reinforcement
d'	= distance from extreme compression fiber to centroid of longitudinal compression reinforcement
d_p	= distance from extreme compression fiber to centroid of prestressing steel
E_c	= modulus of elasticity of concrete
E_p	= modulus of elasticity of prestressing steel
E_s	= modulus of elasticity of reinforcement and structural steel
f'_c	= specified compressive strength of concrete
f_{pe}	= compressive stress in concrete due to effective prestressing force only (after allowance for all prestress losses)
f_{pj}	= jacking stress for pretensioning strands
f_{ps}	= stress in prestressing steel at normal flexural strength
f_{pu}	= specified tensile strength of prestressing steel
f_{py}	= specified yield strength of prestressing steel
f_r	= modulus of rupture of concrete
f_s	= calculated tensile stress in reinforcement at service loads
f_{se}	= effective stress in prestressing steel (after allowance for all prestress losses)
f_t	= extreme fiber stress in tension in the precompressed tensile zone calculated at service loads using gross section properties
f_y	= specified yield strength of reinforcement
h	= overall thickness or height of member
I	= moment of inertia of section about centroidal axis
kd	= distance from extreme fiber to neutral axis
L	= span length of beam
M_e	= moment due to effective prestressing force only (after allowance for all prestress losses)
M_n	= nominal flexural strength at section
P_e	= effective prestressing force (after allowance for all prestress losses)
P_p	= post tensioning jacking force
T_L	= total pretensioning losses
α	= distance coefficient from the end of the bridge girder to the depression point
Δ_{beam}	= deflection due to beam self-weight
Δ_i	= initial camber due to effective pretensioning force

Δ_d = design camber
 ϕ = curvature at a section
 ϕ_c = curvature at midspan
 ϕ_0 = curvature at support

RERERENCES

ACI Committee 318. Building Code Requirements for Structural Concrete (ACI 318-11) and Commentary (318R-11), American Concrete Institute, Farmington Hills, Mich., 2011

Ahmed, S. H, and Shah, S.P., “Structural Properties of High Strength Concrete and Its Implications for Precast Prestressed Concrete,” *PCI Journal*, Feb-March, 1987, pp.130-145

Balant, Z.P., and Panula, L., “Creep and Shrinkage Characterization for Analyzing Prestressed Concrete Structures,” *PCI Journal*, May-June, 1980, pp. 86-122

Barr, P., Kukay, B., and Halling, M., “Comparison of Prestress Losses for a Prestress Concrete Bridge Made with High-Performance Concrete,” *Journal of Bridge Engineering*, V.13, No.5, 2008, pp. 468-475

Barr, P. J., Stanton, J. F., and Eberhard, M. O., “Effects of Temperature Variations on Precast, Prestressed Concrete Bridge Girders,” *Journal of Bridge Engineering*, Vol. 10, No. 2, March/April, 2005, pp. 186-194

Byle, K. A. B., Ned, H., and Carrasquillo, R., (1997). “Time-dependent deformation behavior of prestressed high performance concrete bridge beams,” Center for transportation research bureau of engineering research, University of Texas, Austen, TX, 1997

Choo, Ching Chiaw, (2005). “Investigation of Rectangular Concrete Columns Reinforced or Prestressed With fiber Reinforced Polymer (FRP) Bars or Tendons,” Ph.D. Dissertation, Department of Civil Engineering, University of Kentucky, Lexington, KY, 2005

Ford, J.S., Chang, D.C., and Breen, J.E., "Behavior of Concrete Columns under Controlled Lateral Deformation," *ACI Journal*, V. 78, No. 1, Jan-Feb, 1981, pp. (3-20)

Hognestad, E., "Fundamental Concepts in Ultimate Load Design of Reinforced Concrete Members," *Journal of the American Concrete Institute*, Jun, 1952, pp. 809-830

Hognestad, E., Hansom, N. w., and McHenry, D., "Concrete Stress Distribution in Ultimate Strength Design," *ACI Journal*, V.52, No.6, 1955, pp. 455-480

Holt, E. E., "Early Age Autogenous Shrinkage of Concrete," *Technical research center of Finland*, 2001

Hussien, O.F. et al., "Behavior of Bonded and Unbonded Prestressed Normal and High Strength Concrete Beams," *HBRC Journal*, 2012

Gerges, N., and Gergess, A. N., "Implication of Increased Live Loads on the Design of Precast Concrete Bridge Girders," *PCI Journal*, Fall 2012, pp. 79-95

Jayaseelan, H., and Russell, B. W., "Prestress losses and the estimation of long-term deflections and camber for prestressed concrete bridges," Final Report, School of Civil Environmental Engineering, Oklahoma State University, 2007

Libby, J., "Modern Prestressed Concrete," Design principles and Construction Methods, 3rd Edition, Van Nostrand Reinhold, New York, NY, 1977

Naaman, A.E., "Prestressed Concrete Analysis and Design, Fundamentals," 2nd Edition, Techno Press 3000, Ann Arbor, Michigan. 2004

Nawy, E.E., "Prestressed Concrete, A Fundamental Approach," 3rd Edition, Prentice Hall, Upper Saddle River, NJ, 2000

Precast and Prestressed Concrete Institute, "PCI Design Handbook, 7th Edition, PCI." Chicago, IL, 2011

Robertson, Ian N., "Prediction of Vertical Deflections for a Long-Span Prestressed Concrete Bridge Structure," *Engineering Structure Journal*, July, 2005, pp. 1820-1827.

Saqan, E, and Rasheed, H., "Simplified Nonlinear Analysis to Compute Neutral Axis Depth in Prestressed Concrete Rectangular Beams," *Journal of the Franklin Institute*, September, 2010, pp. 1588-1604

Sethi, V., "Unbonded Monostrands for Camber Adjustment," MS Thesis, Virginia Polytechnic Institute and State University, Blacksburg, VA, 2006

Texas Department of Transportation, "Prestressed Concrete I-Beam and TxGirder Haunch Design Guide." Austen, TX, 2010

Zonaa, Al., Ragni, L., and Dall'Asta, A., "Simplified Method for the Analysis of Externally Prestressed Steel_Concrete Composite Beams," *Journal of Constructional Steel Research*, V. 65, No. 2, February, 2009, pp. 308-313

VITA

Name: Osamah Ibrahim Mahmood

Place of Birth (City, State, Country): Sammarah, Sallah Aldin, Iraq

Education: B.S in Civil Engineering (2003-2007)
University of Tikrit
Tikrit, Iraq

M.S in Civil Engineering (2011-2013)
University of Kentucky
Lexington, KY